CENTRAL RESEARCH LIBRARY
[redacted] DOCUMENT COLLECTION
1

**OAK RIDGE NATIONAL LABORATORY**
operated by
UNION CARBIDE CORPORATION
for the
U.S. ATOMIC ENERGY COMMISSION

MARTIN MARIETTA ENERGY SYSYEMS LIBRARIES
3 4456 0323369 5

ORNL-TM-1361

DECLASSIFIED
CLASSIFICATION CHANGED TO:
BY AUTHORITY OF: AEC 4-1-68
BY: E. Rockenmeister 8-7-68

# COMPATIBILITY OF STRUCTURAL MATERIALS WITH BOILING POTASSIUM

J.H. DeVan

CENTRAL RESEARCH LIBRARY
DOCUMENT COLLECTION
LIBRARY LOAN COPY
DO NOT TRANSFER TO ANOTHER PERSON
If you wish someone else to see this document, send in name with document and the library will arrange a loan.

[redacted]

LEGAL NOTICE

This report was prepared as an account of Government sponsored work. Neither the United States, nor the Commission, nor any person acting on behalf of the Commission:

A. Makes any warranty or representation, expressed or implied, with respect to the accuracy, completeness, or usefulness of the information contained in this report, or that the use of any information, apparatus, method, or process disclosed in this report may not infringe privately owned rights; or

B. Assumes any liabilities with respect to the use of, or for damages resulting from the use of any information, apparatus, method, or process disclosed in this report.

As used in the above, "person acting on behalf of the Commission" includes any employee or contractor of the Commission, or employee of such contractor, to the extent that such employee or contractor of the Commission, or employee of such contractor prepares, disseminates, or provides access to, any information pursuant to his employment or contract with the Commission, or his employment with such contractor.

[redacted]

MARTIN MARIETTA ENERGY SYSYEMS LIBRARIES

3 4456 0323369 5

ORNL-TM-1361

Contract No. W-7405-eng-26

Metals and Ceramics Division

# COMPATIBILITY OF STRUCTURAL MATERIALS WITH BOILING POTASSIUM

J. H. DeVan

APRIL 1966

OAK RIDGE NATIONAL LABORATORY
Oak Ridge, Tennessee
operated by
UNION CARBIDE CORPORATION
for the
U.S. ATOMIC ENERGY COMMISSION

[redacted]

[redacted]

[redacted]

[redacted]

[redacted]

[redacted]



CONTENTS

Page

ABSTRACT . . . . . 1

INTRODUCTION . . . . . 1

MATERIALS SELECTION . . . . . 3

Austenitic Stainless Steels . . . . . 4

Nickel- and Cobalt-Base Alloys . . . . . 7

Refractory Metals . . . . . 9

CORROSION MECHANISMS . . . . . 11

Solubility Studies . . . . . 13

Effects of Impurities . . . . . 18

Oxygen . . . . . 18

Carbon . . . . . 19

OPERATING EXPERIENCE WITH NONBOILING SYSTEMS . . . . . 21

CORROSION AND MASS TRANSFER IN BOILING SYSTEMS . . . . . 28

Corrosion Analysis of Recirculating Boiler Systems . . . . . 29

Comparison of Once-Through and Recirculating Boilers . . . . . 32

OPERATING EXPERIENCE WITH CONVENTIONAL ALLOY BOILING SYSTEMS . . . . 33

Refluxing-Capsule Studies . . . . . 33

Natural-Circulation Boiling-Potassium Loops . . . . . 38

Forced-Circulation Boiling-Potassium Loops with Simulated Nozzle-Blade Test Section . . . . . 41

Single-Rod Capsule Tests . . . . . 45

Seven-Rod Boiler System (SPS-1) . . . . . 46

Firerod Heaters . . . . . 48

Boiler Jet Pumps . . . . . 52

Condenser and Condenser Jet Pumps . . . . . 54

Turbine-Driven Pump . . . . . 56

OPERATING EXPERIENCE WITH REFRACTORY METAL BOILING SYSTEMS . . . . . 58

CONCLUSIONS . . . . . 60

[redacted]

[redacted]

# COMPATIBILITY OF STRUCTURAL MATERIALS WITH BOILING POTASSIUM

J. H. DeVan

## ABSTRACT

The suitability of austenitic stainless steels, nickel-base alloys, cobalt-base alloys, and refractory metals for use as structural materials in boiling-potassium systems is examined with particular attention to corrosion and mass transfer. Experience from the ANP, MCR, SNAP-8, SNAP-50, and MPRE programs is summarized and related to the corrosion requirements of a boiling-potassium Rankine-cycle system. This analysis indicates that, in a recirculating boiler with an efficient vapor separator, mass transfer effects will be counter to those in an all-liquid system. Solution will be restricted to the cooler zones and deposition to the hottest zone (i.e., the boiler) as potassium is distilled off and dissolved material is left behind. This hypothesis is evaluated against the data available for boiling-potassium systems, and the results observed are consistent with the hypothesis. Mass transfer rates are notably lower than in all-liquid systems, and in the absence of contamination effects recirculating boilers have shown negligible corrosion.

A review of strength properties, corrosion and mass transfer problems, fabricability, availability, and costs indicates that type 304 is the best suited of the stainless steels for use in the MPRE and should be satisfactory for a design life of 10,000 hr at 1550°F. The relative merits of nickel-base, cobalt-base, and refractory-metal alloys are compared for operation at temperatures above 1550°F. Refractory metals would appear to permit a substantially higher operating temperature and actually pose less in the way of materials development problems than a nickel- or cobalt-base alloy.

## INTRODUCTION

This report surveys the information available on the compatibility of potassium with structural materials selected for the Medium Power Reactor Experiment.[1,2,3] The purpose is to appraise the corrosion and mass transfer properties of this and future Rankine-cycle, boiling-potassium systems.[4,5]

[redacted]

A substantial background of information on the corrosion problems associated with the use of alkali metals at high temperatures (greater than 1400°F) has been derived from the development programs for high-temperature liquid-cooled reactors for military and space applications. Prominent among these programs have been the following.

Aircraft Reactor Experiment (ORNL)
Aircraft Reactor Test (ORNL)
Lithium Cooled Reactor Experiment (CANEL)
Military Compact Reactor (Allison, UNC)
SNAP-8 (AI, AGC)
SNAP-50/SPUR (CANEL, Airesearch)
Medium Power Reactor Experiment (ORNL)

In these programs there has been a concerted effort to define the compatibility properties of three coolants: sodium, NaK, and potassium. As will be shown, the corrosion problems with all of these coolants are closely related. Thus, although this review is aimed specifically at potassium, much sodium and NaK data from the above programs have been incorporated to give a broader background for interpreting and detailing the potassium compatibility picture.

This report begins with a review of the classes of structural materials that have been considered for vessel, piping, and fuel cladding in boiling-potassium systems. The various classes are compared in terms of their general compatibility characteristics and development potential. Next attention is directed to the fundamental corrosion mechanisms operative in liquid-metal systems and to the corrosion experience gained from nonboiling systems above 1400°F. The last portion of the report analyzes the corrosion properties of boiling-potassium systems. It considers the corrosion mechanisms in recirculating and once-through boilers and relates the analysis to the corrosion data that have been acquired from conventional alloy and refractory-metal, boiling-loop systems at ORNL.

[redacted]



## MATERIALS SELECTION

The selection of structural materials for the containment of boiling potassium has been based on a combination of the following factors:

(1) suitable mechanical properties at operating conditions,

(2) compatibility with potassium at elevated temperatures,

(3) resistance to environmental deterioration (air or space),

(4) ease of fabrication, and

(5) ability to withstand high radiation doses.

[redacted]

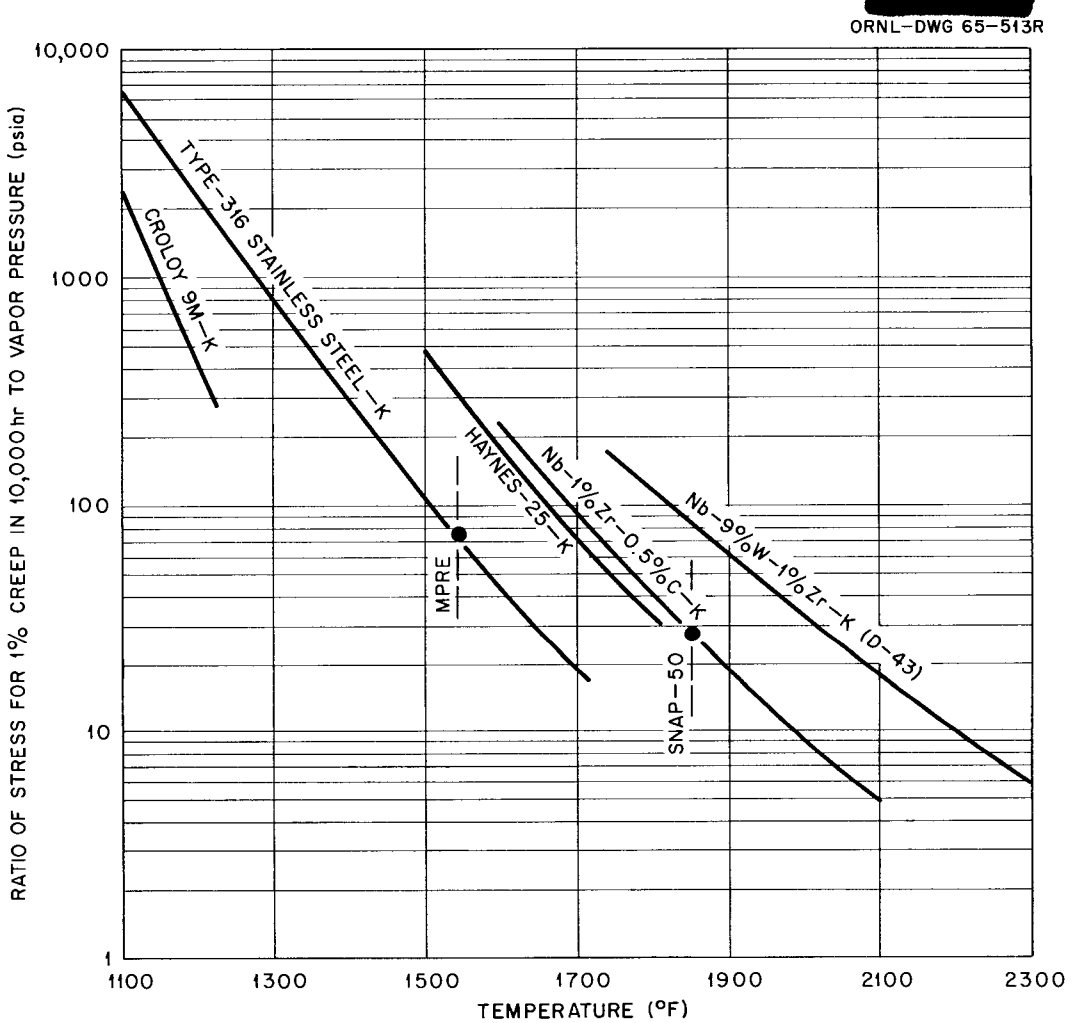


Fig. 1. Effects of Temperature on the Ratio of the Allowable Stress to the Vapor Pressure in the Boiler for Typical Combinations of Materials for Rankine-Cycle Systems.

[redacted]

Materials finding application under these ground rules divide naturally into three classes: austenitic stainless steels, nickel- or cobalt-base superalloys, and refractory metals. The relative strength properties afforded by these alloys for boiling-potassium service are compared in Fig. 1. The comparison is based on the ratio of allowable stress for 1% creep in 10,000 hr to the potassium vapor pressure. Since the forces acting on the boiler and piping walls are largely governed by the vapor pressure, this ratio indicates the relative section thicknesses required for a given safety factor at each temperature. Note that the temperature dependence of creep strength and vapor pressure causes their ratio to fall off very rapidly as temperature increases. The mechanical properties of stainless steels impose a practical temperature limit of about 1550°F for extended operation in a system like the MPRE.[6,7,8] The cobalt-base Haynes alloy No. 25 shows promise for service to 1700°F, and refractory metals show promise to temperatures above 2000°F.

## Austenitic Stainless Steels

The austenitic stainless steels, specifically AISE types 304 and 316, have found extensive application[9] in alkali-metal cooled heat transfer systems operating between 600 and 1300°F. As a class, these alloys offer special advantages in terms of cost, ease of testing, and ease of fabrication. Type 316 stainless steel has been used to the exclusion of other grades for elevated-temperature, liquid-metal applications because until 1965 the ASME pressure vessel code credited it with greater strength at temperatures above 1200°F. Stabilized grades such as types 321 and 347 stainless steels have recently received attention as containment materials for high-temperature alkali metals because tests in association with refractory metals have shown these stabilized grades to be potentially more resistant to decarburization in potassium.[10,11,12] However, they are subject to weld aging phenomena, which have caused difficulty in high-temperature applications.[13,14] Changes in the ASME pressure vessel code now pending give type 304 stainless steel essentailly the same strength as type 316 stainless steel at temperatures above 1200°F. Since type 316

stainless steel is more susceptible to sigma-phase formation, which may be a factor in high-temperature embrittlement, and it has somewhat poorer oxidation characteristics, type 304 stainless steel was selected in the spring of 1965 for the MPRE.

In its formative stage, the MPRE design was predicated on stainless steel corrosion data from the following sources: the High-Temperature Materials Program (ORNL),[15] the Aircraft Nuclear Propulsion Project,[16] the U. K. fast breeder program,[17] and Russian work.[18] Much additional corrosion data have since become available from the Military Compact Reactor Program[12,19] as well as from the MPRE Program. These data show that, with the exception of carbon stability, the above-mentioned 18-8 stainless steel grades are comparable in their resistance to attack by sodium and potassium. The corrosion rates measured for these materials between 1200 and 1650°F are indicated in Fig. 2. The data shown are for nonboiling pumped loop experiments[12,16–25] carried out with sodium, Nak, and potassium. Data from boiling-potassium systems at 1600°F have also been included for comparison. The corrosion rates fall generally within the range 0.2 to 2 mg $cm^{-2}$ $month^{-1}$, which is equivalent to the uniform removal of 0.1 to 1.0 mil thickness of material per year. However, sufficient intergranular penetration may occur above 1500°F to affect the strength of thin fuel cladding. Moreover, the weight losses plotted in Fig. 2 reflect preferential removal of chromium, nickel, and carbon, which while minor in terms of material lost could materially affect the mechanical properties of these steels. Attack of these alloys may also be accelerated by the presence of oxygen, as discussed in the next section.

Although the operating conditions of the various loop tests plotted in Fig. 2 are not directly comparable, there is some evidence that the slightly lower mass transfer rates observed for potassium do represent a real effect. The corrosion properties of sodium and potassium were directly compared by United Nuclear Corporation[26] using identical type 316 stainless steel thermal-convection loops operating at 1575°F. Weight changes of insert specimens at the hottest point in each experiment are reproduced in Fig. 3. Corrosion rates were lower in the potassium loop

[redacted]



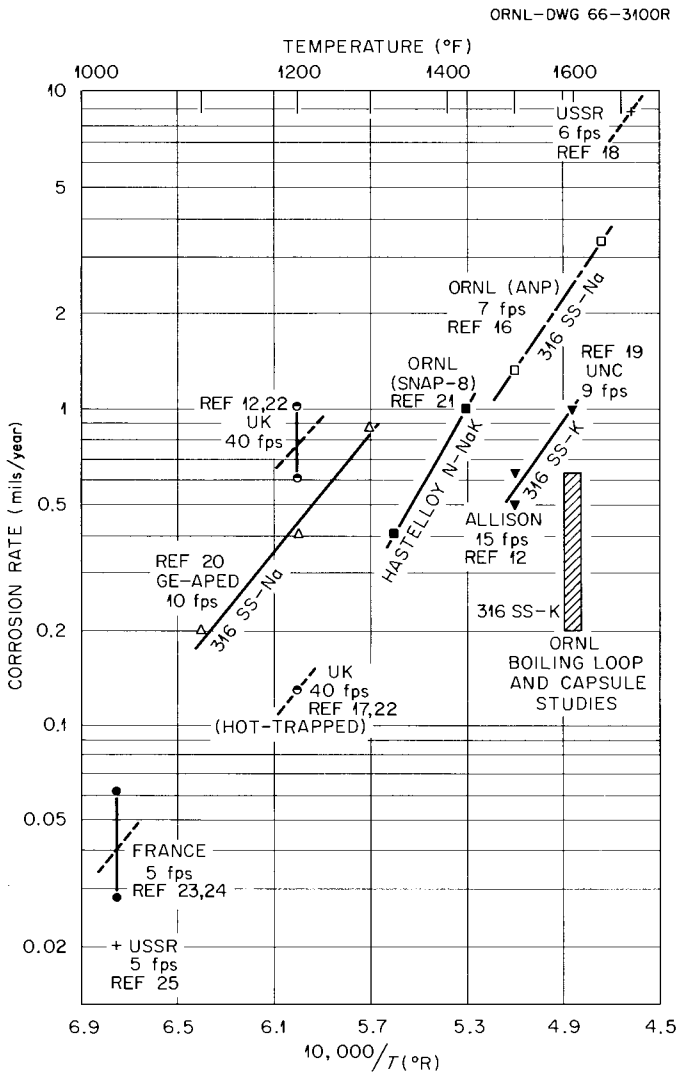


Fig. 2. Relative Corrosion Rates of Stainless Steels in Sodium and Potassium.

than in the sodium loop throughout the 5000-hr test exposures; however, the compositional changes effected in the stainless steel were quite similar for both coolants.

In summary, the corrosion effects of low-oxygen sodium or potassium on stainless steels in the range 1400 to 1600°F have significance in a microscopic rather than a macroscopic sense. That is, manifestations of the corrosion process are normally invisible to the unaided eye. Nevertheless, the microscopic effects (intergranular attack and compositional changes) require close scrutiny when stainless steels are selected for

[redacted]

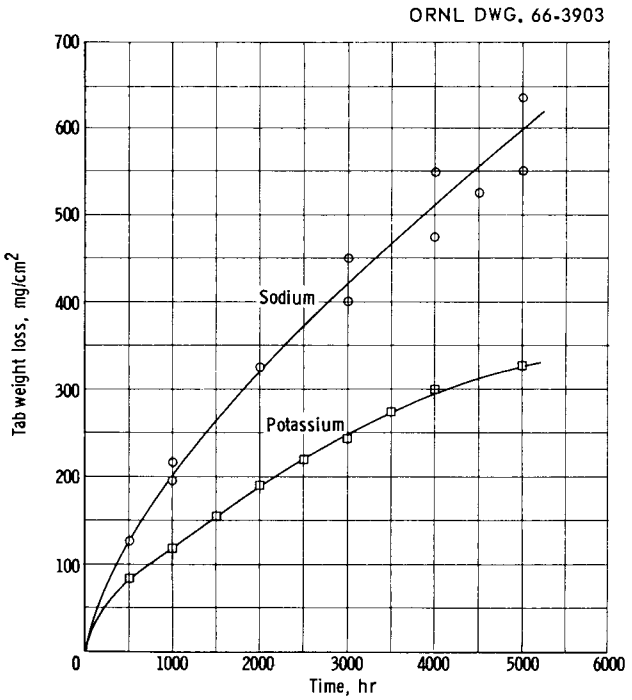


Fig. 3. Sodium-Potassium Corrosion Comparison. Tab weight loss vs time for type 316 stainless steel tabs suspended in sodium and potassium flowing in identical stainless steel thermal-convection loops at 1575°F (475°F ΔT). (Ref. 26)

reactor plant operation. The selection of type 304 stainless steel as the MPRE container material was predicated on the low operating stress levels[6,8] and modest corrosion requirements of the system. As discussed in the last section of this report, operating experience to date attests to the adequacy of this alloy for MPRE service conditions. These conditions, however, are close to the maximum that are practical with stainless steels.

## Nickel- and Cobalt-Base Alloys

The mechanical properties of certain of the nickel- and cobalt-base alloys* would permit a 100 to 200°F increase in the operating temperature of the boiling-potassium reactor system over the maximum temperature level

*Hastelloy X, René 41, Haynes alloy No. 25, Inconel 625.

practicable with austenitic stainless steels. Since these "superalloys" derive their strength from age-hardening reactions, they impose potential fabrication and operational difficulties. Notwithstanding, these materials have drawn some interest both for fuel cladding and vessel applications in assessing the growth potential of the MPRE system.

The corrosion properties of nickel-base alloys have been investigated extensively in sodium and NaK above 1300°F. Principal sources of data include the Aircraft Nuclear Propulsion Program,[16] the SNAP-8 development program,[21] and Russian work.[18] These studies have shown that nickel-base alloys, like austenitic stainless steels, undergo negligible corrosion in sodium or NaK below 1300°F. However, in sodium, NaK, and potassium at higher temperatures the nickel-base alloys are more susceptible to temperature-gradient mass transfer than are the iron-base alloys. Although their corrosion rates increase more rapidly with temperature, the resultant attack tends to be quite uniform without serious pitting or intergranular fissuring. Hence, flow restrictions stemming from the growth of mass transfer deposits are a more troublesome problem than reductions in tube wall thickness.

The available data on nickel-base alloys relate almost entirely to nonboiling systems. As explained in the next section, corrosion requirements of boiling and nonboiling systems differ significantly. Thus, the mass transfer tendencies that nickel-base alloys show in polythermal all-liquid loops do not a priori carry over to a two-phase boiling system. It is also significant that nickel-base alloys are much less affected by oxide contamination in sodium than are iron-base alloys.[16,22] Hence, nickel-base systems permit a much greater latitude in purity control than do stainless steels, particularly above 1400°F.

The corrosion properties of cobalt-base alloys in either sodium or potassium are not at present well documented. Theoretical considerations indicate that cobalt should resist dissolutive attack by these liquid metals to at least the same degree as iron and better than nickel. In two loop experiments of Haynes alloy No. 25 conducted with boiling potassium,[27]

corrosion rates at 1600°F were equivalent to those of type 316 stainless steel at similar temperatures. Furthermore, weight losses of Haynes alloy No. 25 at an 1800°F boiling-condensing temperature were not significantly higher than at 1600°F. Thus cobalt-base alloys show considerable promise as an MPRE container material for service above 1540°F.

## Refractory Metals

Refractory metals probably provide the ultimate in properties for advanced high-temperature, alkali-metal systems. They are more resistant to dissolutive attack than conventional metals, and their strength is retained to the temperature region above 2000°F, where conventional alloys cease to be useful engineering materials. Furthermore, their commercial availability in forms useful to engineering systems has burgeoned in recent years.

The primary disadvantage of refractory metals for vessel and piping applications lies in their susceptibility to air oxidation. This, of course, is not a detriment in the rarified atmosphere of space; however, much expense is entailed in development tests that require the simulation of space environment. Another limitation arises from the relatively high chemical affinity of refractory metals for carbon and nitrogen. Thus, dissimilar-metal mass transfer problems are encountered if refractory metals are combined with conventional alloys or, in certain cases, with other refractory metals.

The presence of oxygen in alkali metals is quite deleterious to most of the refractory metals.[28] In fact, the mechanism of corrosion of these metals in either sodium or potassium clearly seems to be oxygen controlled.[17,28,29,30] At lower temperatures (<1400°F) in oxygen-contaminated sodium, alloys of niobium, vanadium, and tantalum suffer excessive weight loss owing to formation of nonadherent oxides. At higher temperatures oxygen partitioning between alkali metals and refractory metals may also lead to diffusion of oxygen into the base metal, with a serious reduction in ductility. The use of refractory metals in potassium depends, therefore, on keeping the oxygen content of the liquid metal at an absolute minimum (e.g., by zirconium hot-trapping).

In the absence of oxygen, refractory metals show extremely low rates of corrosion in either sodium or potassium. Loop studies of both coolants,[31,32] conducted at temperatures as high as 2200°F, have shown negligible mass transfer of niobium-, tantalum-, and molybdenum-base alloys after periods as long as 5000 hr. If used in combination with conventional alloys, however, refractory metals are subject to carburization and nitriding.[11,33] These phenomena are normally manifested by the formation of a carbide-nitride layer on the refractory metal and by decarburization and, in some cases, nitrogen depletion of the conventional alloy. At ORNL the extent of transport of carbon and nitrogen occurring between niobium and 316 stainless steel in sodium-filled capsules was examined[33] at temperatures from 1500 to 1800°F for up to 1000 hr. The migration of carbon and nitrogen to the niobium alloys increased with time, temperature, and stainless steel-to-niobium surface ratio. In tests at 1800°F in which the niobium surface area was 10 times that of stainless steel, niobium transfer to the stainless steel was also observed. Niobium specimens after test exhibited brittle surface layers identified as NbC and NbN. Carbon was found to be principally in this layer, but nitrogen had penetrated the entire 0.090-in. specimen thickness. The niobium significantly increased in ultimate tensile strength and decreased in percent elongation in tensile tests both at room temperature and at 1800°F.

Limited data on molybdenum alloys indicate that the problem of interstitial transport is less severe for this alloy system in contact with conventional alloys than for niobium and tantalum alloys. In a type 316 stainless steel capsule[29] containing potassium and TZM alloy (Mo–0.5% Ti–0.08% Zr), operated at ORNL for 500 hr at 1800°F, heat treatment or exposure caused no significant changes in the interstitial content of the TZM alloy and no change in its tensile strength.[33] Also, molybdenum alloys seem to tend less to getter oxygen from sodium or potassium than do tantalum or niobium alloys.

In the selection of refractory metals for potassium service, corrosion would appear to be a deciding factor only where oxygen contamination is expected or where the refractory alloys are to be used

in combination with conventional alloys. Otherwise, the alloy classes tested to date, which include tantalum-, niobium-, and molybdenum-base systems, all have demonstrated exceptional resistance to dissolutive or mass transfer attack in potassium.

Of the three classes of structural materials discussed in this section, refractory metals show by far the greatest system growth potential. In fact, the use of refractory metals for a boiling-potassium system at this time poses fewer unanswered development questions than the use of either a nickel- or cobalt-base alloy. Furthermore, the payoff with refractory metals, considering strength, compatibility, and metallurgical stability, should be greater in terms of both the ultimate temperature limits and reliability. Of the currently developed refractory metals, the tantalum-base alloy T-111 (Ta–8% Hf–2% W) shows particular promise[34] as a container material for boiling potassium in the range 2000 to 2200°F. Other tantalum-base alloys now in the development stage promise still further increases in system temperature. The ultimate limit of boiling-potassium systems is not definable at present but must await further studies of these advanced tantalum alloys as well as more exotic tungsten-base alloys.

## CORROSION MECHANISMS

The corrosion properties of liquid alkali metals have been under systematic investigation since 1946. Manly[35] noted the corrosion processes in liquid metals to be of two principal types:

1. simple solution leading to general surface removal, grain boundary attack, or preferential leaching of alloying constituents;
2. chemical attack involving impurities in the liquid metal and in or on the container wall.

As a further consequence of either of these corrosion processes, elements of the container metal may undergo continual transport from one part of a dynamic system to another. Two factors contributing to this mass transfer are (a) solubility differences resulting from temperature gradients in the system and (b) activity differences resulting from dissimilar

metals in the system. Since equilibrium solubilities in liquid metals nearly always change with temperature, temperature-gradient mass transfer is an inevitable side effect of any high-temperature, liquid-metal, thermal- or forced-convection system. Dissimilar-metal mass transfer, on the other hand, can be minimized through the selection of system materials that are not prone to interalloying.

Theoretical treatments of the kinetics of dissolution of solids in liquids have been developed from studies of the solution of inorganic and organic salts in water and nonaqueous solvents.[36] The overall rate of dissolution is traced mechanistically to two sequential transfer steps:

1. the net rate at which solute atoms escape from the solid surface into the liquid layer immediately against the solid,
2. the rate at which the solute atoms diffuse from this liquid layer into the bulk liquid.

Combining the rate equations for both steps leads to an overall rate expression[37]

$$J = K(C_{eq} - C) \quad , \tag{1}$$

where

$J$ = mass of solute transferring into the liquid per unit time per unit surface area,

$C_{eq}$ = saturation concentration of solute in liquid,

$C$ = bulk concentration of solute in liquid,

$K$ = solution rate constant = $f(T)$.

From this expression it is evident that the rate of dissolution at any given point in a liquid-metal circuit will be controlled by the <u>degree of undersaturation</u> of the solute at that point and by a temperature-dependent rate constant.

In nonisothermal systems, the overall mass transfer rate is a function not only of solution rates but also of deposition rates. Although less is known regarding the kinetics of the deposition process,

both temperature and the degree of oversaturation play commanding roles. In loop studies conducted with type 316 stainless steel and sodium at 1500°F, Holman[38] found the rates of solution and deposition to be equivalent for the same absolute concentration driving force and temperature.

## Solubility Studies

In general, the solubilities in alkali metals of elements making up our useful high-temperature structural alloys are relatively low. Theoretical predictions by Strauss *et al.*[39] and measurements in lithium by Leavenworth and Cleary[40] suggest that both solubility and the temperature coefficient of solubility depend strongly on the disparity in the atomic radii of solvent and solute atoms. Since the size factor is large between alkali metals and the container metals of interest, their mutual solubility should be small. The Hildebrand model,[41] which considers the available free volume in a liquid, affords another approach to solubility predictions. Using the Hildebrand formula, Swisher[42] calculated the solubilities of iron, nickel, and cobalt in potassium and compared them with experimental values. His results are shown in Table 1 and indicate poor agreement between the

Table 1. Experimental and Theoretical Solubility and Heats of Solution of Iron, Nickel, and Cobalt in Potassium at 1000°K(1340°F). (Ref. 42)

| Solute | Experimental Solubility[a] (ppm) | Experimental Heat of Solution (kcal/mole) | Hildebrand Model Solubility[a] (ppm) | Hildebrand Model Heat of Solution (kcal/mole) |
|---|---|---|---|---|
| Iron | 75.0 | 28.2 | $10^{-8}$ | 64.3 |
| Nickel | 4.6 | 13.9 | $10^{-10}$ | 71.6 |
| Cobalt | <5.0 | | $10^{-10}$ | 73.1 |

[a]Atomic parts per million.

calculated and experimental results; however, the Hildebrand model does not take into account any complex bonding that may occur between solute and solvent and, more importantly, any bonding arising from the presence of impurity elements.

A long-term interest in iron-base alloys for alkali-metal heat transfer circuits has stimulated a number of independent investigations of the solubility of iron in sodium and potassium. Figure 4 compares data resulting from the early studies of iron in sodium[43,44] and more recent work on iron in potassium.[42,45,46] (The straight lines for this plot have been forced by iterating what appear to be the most reasonable data points.) Although the slopes of the two curves for potassium are nearly equivalent, they are shifted by an order of magnitude. It is beyond the scope of this report to discuss the experimental errors involved in developing solubility data for alkali metals, but it may suffice to say that the pitfalls are many and can easily account for the disagreement between the curves. For example, Swisher found that the observed solubility of iron in potassium varied by two orders of magnitude depending on the metal selected for his sampling cup.[42] (The data in Fig. 4 represent the solubility values determined with a molybdenum cup.) He further attributed the higher iron concentrations in his experiments compared to those of McKisson and Eichelberger[45] to oxide impurities in the potassium.

Several workers have examined the solubility of nickel and refractory metals in potassium.[42,45–48] The data are summarized in Table 2. In general, the reported solubilities have been in the range 10 to 100 ppm, but substantially higher solubilities have resulted where oxygen impurities existed in either the potassium or container metal.

There is obvious difficulty in applying the available solubility data for potassium to a worthwhile corrosion rate analysis. Besides the difficulty in selecting an appropriate solubility curve for the pure metals, there is the question of the solubilities of the constituents of an alloy relative to the solubilities of the pure metals. Also data are not available on solution rate constants, which are essential to predicting mass

[redacted]



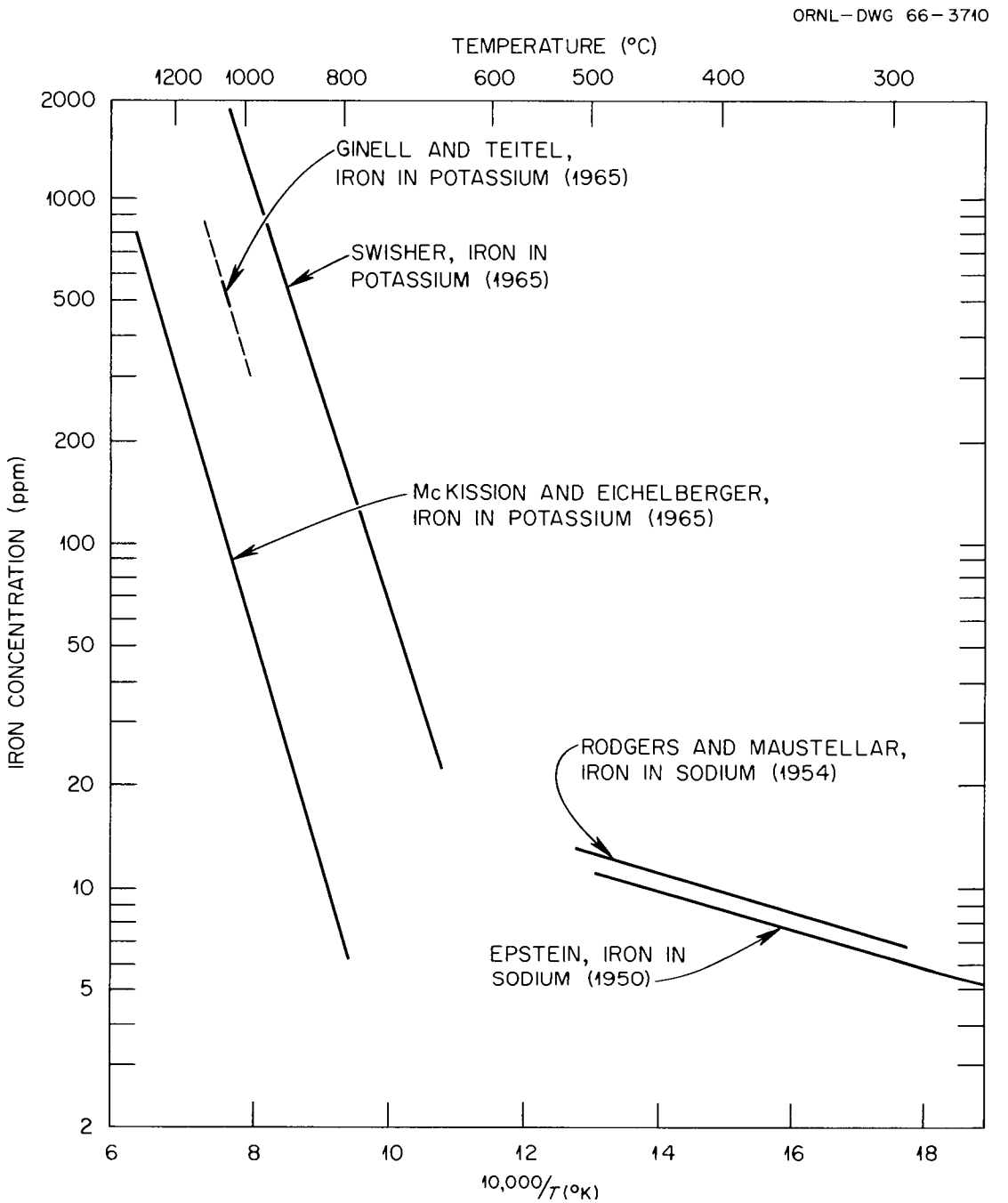


Fig. 4. Solubility of Iron in Sodium and Potassium.

[redacted]

Table 2. Solubilities of Nickel, Molybdenum, Tantalum, and Niobium in Potassium

| Solute Element | Temperature (°F) | Equilibration Time (hr) | Measured Solute Concentration (ppm) | Oxygen Concentration in Potassium (ppm) | Reference |
|---|---|---|---|---|---|
| Nickel | 1230 | not given | 8 | < 20[a] | 42 |
| | 1390 | not given | 10 | < 20[a] | 42 |
| | 1590 | not given | 25 | < 20[a] | 42 |
| | 1810 | not given | 35 | < 20[a] | 42 |
| | 1930 | not given | 85 | < 20[a] | 42 |
| | 1690 | 5–10 | 3,4,5 | 10[a] | 46 |
| | 1830 | 5–10 | 4,115 | 10[a] | 46 |
| Molybdenum | ≤ 2200 | 100 | < 0.2 | 25[a] | 47 |
| | 1300–2200 | 100 | 500 | 500[b] | 47 |
| | 1830 | 4–8 | 2,3,4 | 14[a] | 45 |
| | 2010 | 8 | 1,17 | 14[a] | 45 |
| | 2190 | 8 | 8,13,14 | 14[a] | 45 |
| Tantalum | 2065 | 5 | 17 | 23[a] | 46 |
| | 2270 | 10 | 125,150 | 10[a] | 46 |
| | 2425 | 5 | 6,15,115 | 23[a] | 46 |
| Niobium | 750 | 48 | 35,125,135 | 50[c] | 48 |
| | 1110 | 48 | 140,150 | 50[c] | 48 |
| | 1470 | 48 | 375 | 50[c] | 48 |
| | 1500 | 48 | 405 | 50[c] | 48 |
| | 1400 | 100 | 40,140,410 | 25[a] | 47 |
| | 1800 | 100 | 40,95 | 25[a] | 47 |
| | 2000 | 100 | 6,65,100,935 | 25[a] | 47 |
| | 2100 | 100 | 160 | 25[a] | 47 |
| | 2200 | 100 | 15,35 | 25[a] | 47 |

Table 2 (continued)

| Solute Element | Temperature (°F) | Equilibration Time (hr) | Measured Solute Concentration (ppm) | Oxygen Concentration in Potassium (ppm) | Reference |
|---|---|---|---|---|---|
| Niobium | 1830 | 8 | 15 | 14[a] | 45 |
| | 2010 | 8 | 12 | 14[a] | 45 |
| | 2190 | 8 | 34 | 14[a] | 45 |
| | 2065 | 5 | 10 | 23[a] | 46 |
| | 2235 | 5 | 9,28 | 23[a] | 46 |
| | 2270 | 10 | 7,13,14 | 10[a] | 46 |
| | 2425 | 5 | 31 | 23[a] | 46 |

[a]Amalgamation method.

[b]Oxygen added as $KO_2$.

[c]Zirconium gettering-vacuum fusion.

transfer rates. Discussions to follow assume that iron solubilities of the magnitude found by Swisher[42] will generally apply to the boiler region of any iron-base alloy and that the data of McKisson and Eichelberger[45] will be more applicable to the condenser and condensate return areas.

## Effects of Impurities

### Oxygen

The oxygen content of sodium and potassium has a major effect on the rate of corrosion and mass transfer of transition metals. Tyzack[49] explains the behavior of transition elements in an oxygen-sodium system by considering the relative stabilities of the system oxides. He points out that the oxide of the solid metal will be reduced when it is thermodynamically less stable than sodium oxide. Eventually, pure metal will be exposed to the sodium and the extent of corrosion will then depend on dissolution. Iron and nickel have oxides that fall into this class. Transition metals whose oxides are more stable than sodium oxide will oxidize by gettering oxygen from the sodium. Corrosion, in this case, becomes a function of the "passivity" of the solid-metal oxide which, in turn, depends on the adherence and vacancy density of the oxide film. Uranium and zirconium are in this category. A third class of transition metals has oxides of stability comparable to that of sodium oxide. Tyzack predicts that this group, which includes Cr, Nb, V, and Ta, should form complex oxides with sodium and oxygen. The mechanism of corrosion for this class of materials is less well understood. However, the complex oxides are generally unprotective.

There is increasing evidence that the formation of complex oxides plays a dominant role even in the case of transition metals with relatively low oxide stabilities. The expanding list of double oxides now identified or suspected in sodium and potassium systems include $Na_2FeO_2$ (ref. 50), $Na_4FeO_3$ (ref. 51), $NaCrO_2$ (refs. 21, 52), $Na_8Nb_2O_9$ (ref. 53), $Na_2Nb_2O_5$ (ref. 49), $Na_3NbO_4$ (ref. 54), $K_2MoO_4$ (refs. 47, 55), and $KNbO_3$ (ref. 48). The absence of any nickel compounds from this list is particularly significant in view of the reported immunity of this element to effects of oxygen in sodium and NaK.

At higher temperatures, oxygen effects may be manifested not only by accelerated corrosion but also by the partitioning of oxygen between the container metal and liquid metal. This latter phenomenon is particularly important in the case of tantalum and niobium, which may become embrittled by the uptake of oxygen from even relatively pure (i.e., cold-trapped) sodium.

Oxide impurities are more easily controlled in sodium than in potassium. As shown in Fig. 5, the saturation values for oxygen in potassium are almost two orders of magnitude greater than in sodium. Thus, unlike in sodium, low oxygen levels in potassium cannot be achieved by cold trapping or filtering. Instead, purification techniques must depend on vacuum distillation of the potassium prior to use or hot trapping with an active metal such as zirconium.

Recent studies at ORNL have shown that the rate of oxygen uptake by zirconium in potassium can be correlated with a diffusion model for oxygen movement through the zirconium.[56] These studies have afforded a quantitative basis for the design of hot traps for potassium systems. This work also demonstrated that the distribution ratio for oxygen between zirconium and potassium was sufficiently reproducible to afford a useful analytical procedure for the determination of oxygen in potassium. This analytical procedure, termed the gettering-vacuum fusion (GVF) method, allows an accurate determination of the total oxygen content of potassium even in the presence of corrosion products. The newly developed electrochemical meter[9] also appears to be an effective device for monitoring the oxide content of potassium.

## Carbon

Carbon contamination in liquid potassium or sodium circuits may have important consequences with respect to carburization or corrosion reactions. The exact form of carbon impurities in potassium or sodium has been the subject of much debate in recent years. Despite earlier predictions that dissolved carbon should exist in elemental form, Russian workers have indicated that it may be present in sodium as a monoxide.[57]

[redacted]



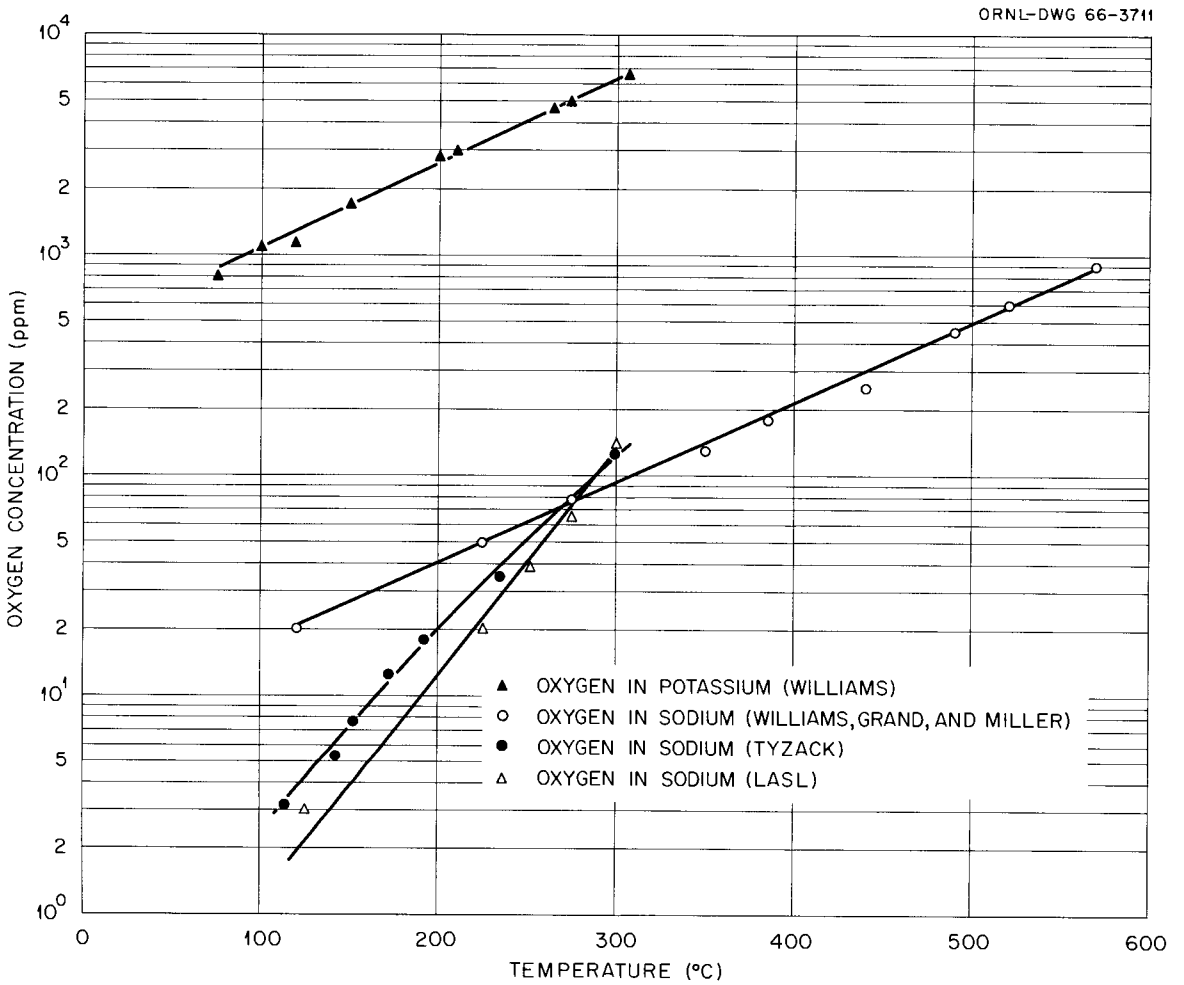


Fig. 5. Solubility of Oxygen in Sodium and Potassium. (Refs. 59, 60, 61, and 62).

[redacted]

In any case, carbon impurities from sodium and potassium will react with stainless steel and diffuse into it. The depth of carburization depends on the magnitude of the resultant carbon concentration gradient, which in turn depends on the reaction rates and solid-state diffusion rates of carbon in stainless steel. Studies of the carburization rates of type 304 stainless steel have been reported for sodium systems as a function of both temperature and carbon content of the sodium.[58] Similar data are unavailable for potassium.

Carbon contamination in liquid-metal-cooled reactor plants comes principally from organic coolants and lubricating oils. Since these sources are conspicuously absent from the MPRE and its engineering mock-ups, changes in carbon concentration as a consequence of impurities in these systems are considered unlikely. Nevertheless, carbon transport may arise from temperature gradients in the system. These effects are discussed in a later section.

## OPERATING EXPERIENCE WITH NONBOILING SYSTEMS

Liquid sodium and sodium-potassium alloys have been used for many years in graphite-moderated and fast breeder reactor plants having maximum liquid-metal temperatures of 600 to 1000°F. More recent adaptations of sodium cooling to fast breeder reactors have extended this temperature range to 1300°F. Two excellent reviews[9,17] of the materials technology associated with these reactor plants have recently been published, and only passing mention of these systems need be made here.

Though less publicized, an impressive backlog of alkali-metal technology above 1300°F has grown out of the development of nuclear reactors for military and space applications. For the most part this experience has been derived from nonnuclear corrosion and heat transfer systems operated in the development programs for these reactors. Sources of corrosion data of use to the MPRE program are listed in Table 3 together with reference temperatures and containment materials.

Table 3. High-Temperature Reactor Development Programs Using Sodium, NaK, or Potassium Coolants

| Reactor Designation | Development Sites | Liquid Metal | Fuel Element Cladding | Pipe and Vessel Materials | Maximum System Temperature (°F) |
|---|---|---|---|---|---|
| Aircraft Reactor Experiment | ORNL | Sodium (Reflector Coolant) | | Inconel | 1500 |
| Aircraft Reactor Test | ORNL, P&W,[a] BMI[a] | Sodium (Reflector Coolant) NaK (Secondary Coolant) | | Inconel | 1600 |
| Military Compact Reactor | Allison Division, United Nuclear | Potassium | Nb–1% Zr | Type 316 Stainless Steel | 1600 |
| SNAP-8 | AGC, AI | NaK | Hastelloy N | Types 316 and 347 Stainless Steel, Hastelloy C, Croloy 9M | 1300 to 1400 |

[a]Conducted supporting corrosion studies.

The conceptual design work on the MPRE was carried out on the basis of the corrosion information obtained for alkali metals in the 1500 to 1600°F temperature range in the course of the Aircraft Nuclear Propulsion program[16] conducted during the 1950's. Studies at ORNL using sodium and NaK in this temperature range included 65,000 hr testing of 500-kw to 1-Mw heat exchangers and 74,000 hr of forced-convection corrosion loop testing.

The basic loop design employed for corrosion studies is shown in Fig. 6. Oxide purity was maintained by a circulating bypass cold trap connected in parallel with the loop. Flow rates in the system were held in the range 7 to 15 ft/sec (1.5 to 3.0 gal/min). Mass transfer rates were determined by weighing all material transported to the cold-leg regions of the loop.

The results of monometallic loop tests carried out with various alloys under this program are compared in Fig. 7. All loops in this series were operated for 1000 hr with a 300°F cold-trap temperature. Comparisons of the amount of cold-leg deposition showed that types 304, 316, and 347 stainless steels were considerably more resistant to mass transfer at 1500°F than other stainless steels or nickel-base alloys. The mass transfer rate of Inconel X was slightly lower than that of Inconel at 1500°F, while that of Hastelloy B was slightly higher. The appearance of hot-leg specimens from types 304 and 316 stainless steel loops is shown in Fig. 8. Examination of these specimens showed a limited amount of intergranular attack (0.2 to 0.5 mil). Also a shallow region (1 to 5 mils) below the exposed surface was partially depleted of carbon, nickel, and chromium. Bend tests and hardness measurements on these specimens, however, indicated no discernible effects of sodium exposure.

Similar tests were more recently completed with potassium under the auspices of the Military Compact Reactor Program. Table 4 lists the corrosion loops operated and examined at both the Allison Division[12] and the United Nuclear Corporation.[19] The purpose of these corrosion tests was to predict the performance of a potassium-cooled reactor plant using Nb–1% Zr as the fuel cladding and type 316 stainless steel as the primary

[redacted]



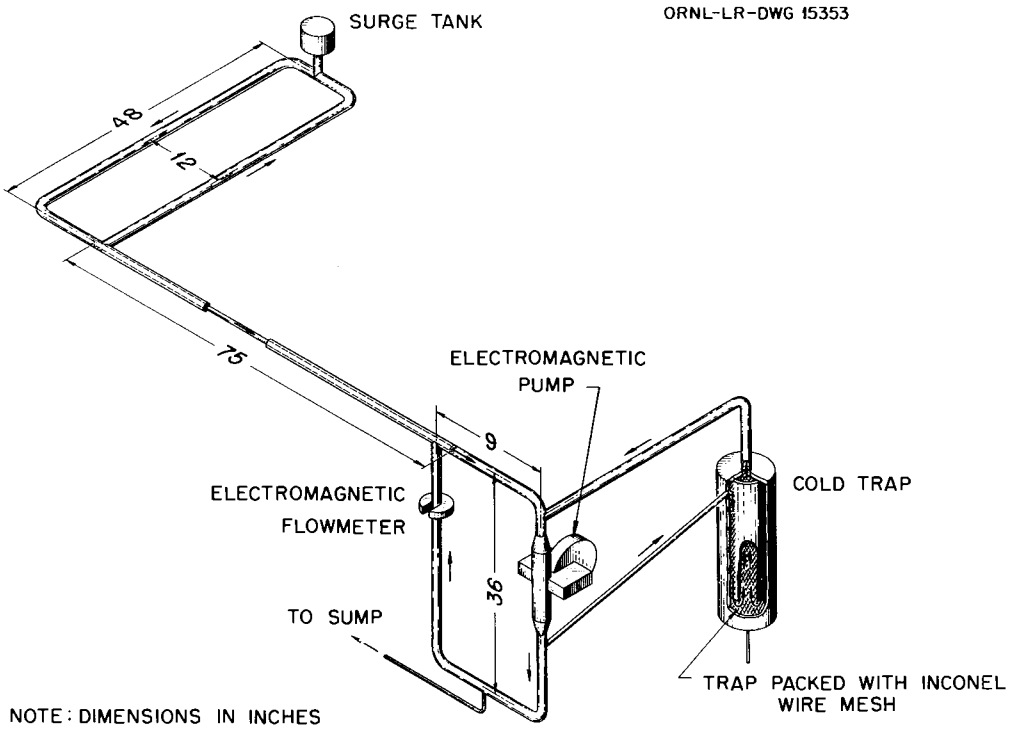


Fig. 6. Basic Design of Loops Used in ORNL ANP Program Corrosion Studies.

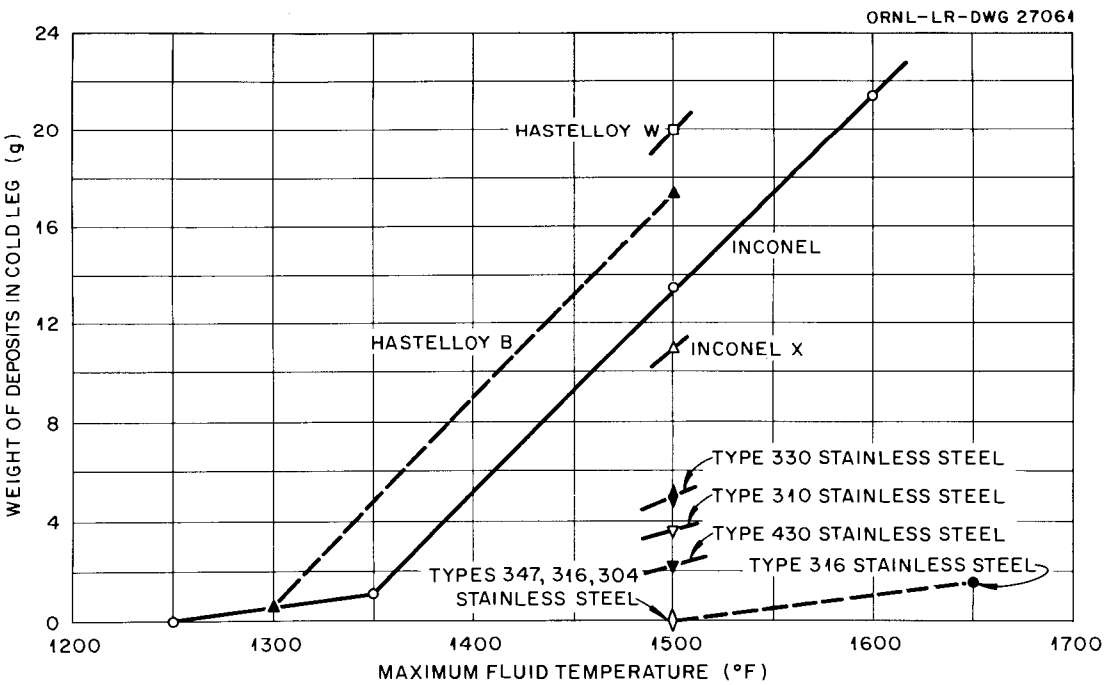


Fig. 7. Mass Transfer Observed in ANP Pumped Loops as a Function of Maximum Temperature.

[redacted]

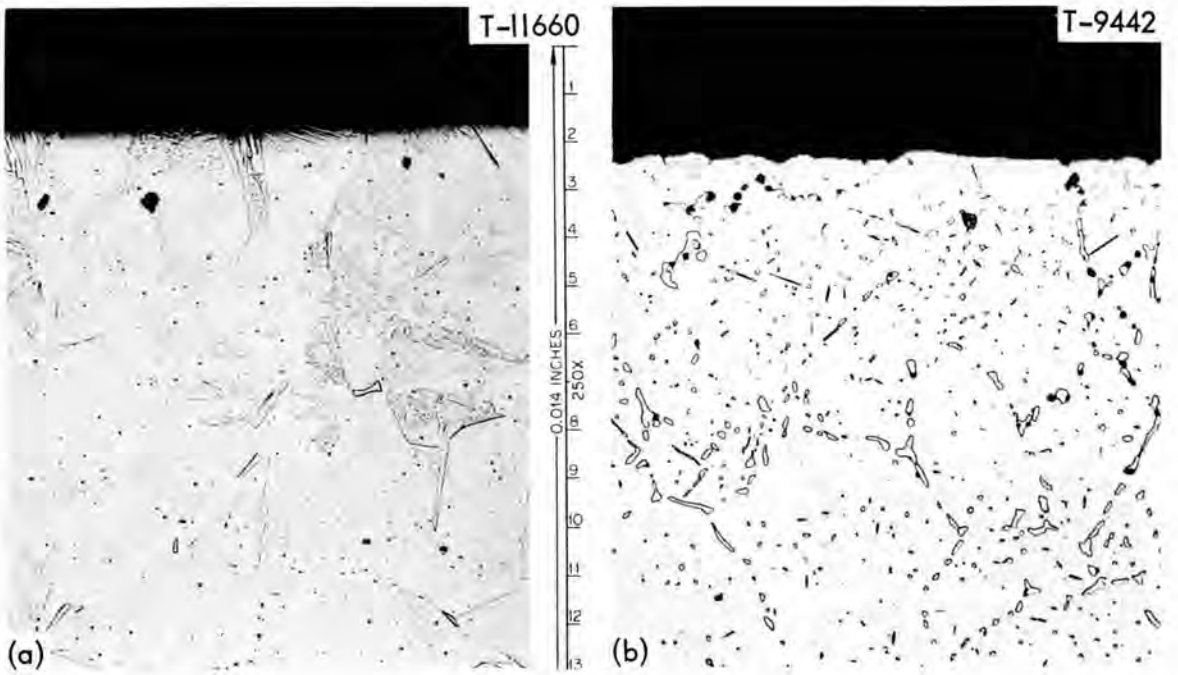


Fig. 8. Metallographic Appearance of Hot-Leg Section of (a) Type 304 Stainless Steel and (b) Type 316 Stainless Steel Forced-Convection Sodium Loops. Loops operated 1000 hr at 1500°F hot-leg temperature, 1200°F cold-leg temperature. Sections were taken from point of maximum loop temperature. Etchant: modified aqua regia. 250X.

containment and structural material. Information collected included weight changes of hot- and cold-leg insert specimens, metallographic examinations, and chemical analyses of the loop walls and insert specimens. Stress-rupture tests at 1500°F were also performed on type 316 stainless steel that had been exposed to loop operation at 1500°F.

Oxygen partitioned rapidly between the potassium and Nb–1% Zr specimens and diffused into the latter. Nitrogen and carbon transferred from the stainless steel to the Nb–1% Zr. Nitrogen diffused into the Nb–1% Zr as deep as 0.024 in. at 1500°F, while carbon was confined to a thin layer on the Nb–1% Zr. Weight changes of Nb–1% Zr specimens at 1500°F were relatively small in low-oxygen systems.

Dissolution of type 316 stainless steel was "moderate and predictable."[12] Rates were particularly sensitive to the oxygen level and fluid velocity. The major corrosion effects on stainless steel

Table 4. Stainless Steel-Potassium Corrosion Loop Studies Conducted Under the MCR Program

| Source | Test System | Flow Rate (ft/sec) | Temperature Maximum (°F) | Temperature Minimum (°F) | Normal Test Duration (hr) | Accumulated Operation (hr) |
|---|---|---|---|---|---|---|
| Allison (Ref 12) | Type 316 stainless steel loop; types 304, 310, 321, 347, 316 stainless steel sleeve inserts | 15 | 1500 | 1200 | 900 | 900 |
| | Type 316 stainless steel loop; type 316 stainless steel and Nb–1% Zr sleeve inserts | 5,15,22 | 1500 | 1200 | 385–4000 | 30,000 |
| UNC (Ref 19) | Type 316 stainless steel loop; type 316 stainless steel and Nb–1% Zr tab inserts | 9 | 1600 | 1200 | 1560 | 1560 |
| | Type 316 stainless steel thermal-convection loop; type 316 stainless steel and Nb–1% Zr tab inserts | 0.5 | 1600 | 1200 | 250–5000 | 100,000 |

specimens were carbon depletion and grain boundary attack. Stress-rupture tests of exposed stainless steel specimens showed lower strengths than unexposed specimens. However, whether this strength loss was related to thermal history or to the effects of potassium *per se* was not determined.

Concurrent with the above research, ORNL investigated the compatibility of several materials of construction for use with NaK in the SNAP-8 primary system. Forced-convection loops were operated with a 1425°F maximum hot-leg temperature and a cold-leg temperature of 1100°F. The loops were basically constructed of type 316 stainless steel, but they incorporated a Hastelloy N heater section and a Croloy 9M cooler section. Data from these loops[21] supported previous findings that 18-8 stainless steels are more resistant than nickel-base alloys to mass transfer in low-oxygen NaK. The opposite was true when the NaK was badly contaminated with oxygen. In low-oxygen NaK, the 18-8 stainless steels showed less than 0.2 mils/year corrosion and no evidence of intergranular attack. However, carbon migrated extensively from Croloy 9M to the other materials. In NaK with very high oxygen content the corrosion rate increased substantially even at 1300°F and resulted in considerable intergranular penetration. Chromium and iron were the two elements most affected by oxygen.

As discussed in the next section, the corrosion rates measured in nonboiling systems are not quantitatively applicable to boiling systems. Nevertheless, the nonboiling loop systems discussed here provide evidence of the types of compatibility problems likely to be experienced with potassium in conventional alloys. The following conclusions drawn from these nonboiling studies have particular significance to the MPRE program.

1. Mass transfer rates of 18-8 stainless steels in high-purity sodium or potassium convective heat transfer systems have been relatively low (< 1 mil/yr), even at 1500°F.

2. Corrosion processes occurring in nonisothermal stainless steel systems above 1200°F are manifested by the migration of C, Ni, Mn, and Cr from the hot to the cold regions. Although the total mass of transferred material is small, the effects of this migration on the mechanical properties of thin structural members may be significant.

3. Intergranular attack is observed in the hottest regions of stainless steel forced-convection heat transfer systems operated with sodium or potassium at 1500°F. The presence of oxygen will induce intergranular attack at temperatures as low as 1200°F and will greatly accelerate intergranular attack at higher temperatures. The extent of intergranular attack does not appear significant for heavy structural members but could affect the load-bearing characteristics of thinner (<0.020 in.) members.

4. Above 1300°F nickel-base alloys are more prone to temperature gradient mass transfer in sodium than are austenitic stainless steels. However, the corrosion rates of nickel alloys appear less affected by oxide impurities in sodium.

## CORROSION AND MASS TRANSFER IN BOILING SYSTEMS

In nonboiling systems, the entry of solute from the wall and its movement from point to point can be expressed as a continuous function of time and position. The addition or removal of heat from the system, since it affects the liquid metal temperature, has a direct influence on the equilibrium concentration and rate constant terms of Eq. (1). The degree of undersaturation and the solution rate constant generally become maximized at the heater outlet, and the maximum corrosion rate is normally encountered at that point.

The situation in a boiling liquid metal circuit is quite different from that described above. First, solute does not flow continuously around the circuit, since, unlike the liquid metal, the vapor-filled regions present a high resistance path to solute mass transfer. Accordingly, concentration changes occurring in the boiler are not directly transmitted downstream from the boiler.

Second, heat addition to potassium at its boiling point produces no discernible change in liquid temperature and, therefore, does not alter either the equilibrium saturation level of the liquid or the solution rate in this region. In fact, heat addition to the boiler liquid fractionates it into pure vapor and impure liquid, concentrating the impurities and causing <u>supersaturation</u> rather than undersaturation.

A third difference between boiling and forced-convection liquid metal systems is to be found in their comparative mass flow rates. Because of the relatively high latent heat of condensation, the mass flow rate required to transport energy at a given rate is considerably less in a boiling system than in a forced-convection circuit. Thus the liquid flow rates and velocities tend to be much lower in boiling systems.

It is interesting to relate these observations to the comparative operating behavior of recirculating boiler systems, such as the MPRE, and "once-through" boilers, in which the liquid is completely dried.

## Corrosion Analysis of Recirculating Boiler Systems

A simplified block diagram of the MPRE system is shown in Fig. 9. Consider first the boiler circuit, consisting of a boiler delivering a low quality (approx 20%) vapor-liquid mixture, a vapor separator, and a jet pump. Potassium entering the boiler at a rate of 5.5 lb/sec is converted to a mixture of 1.1 lb/sec vapor and 4.4 lb/sec liquid. At the vapor separator, the vapor fraction is extracted from the boiler circuit. The liquid fraction is directed into the jet pump, mixed with the condensate return, and sent back to the boiler.

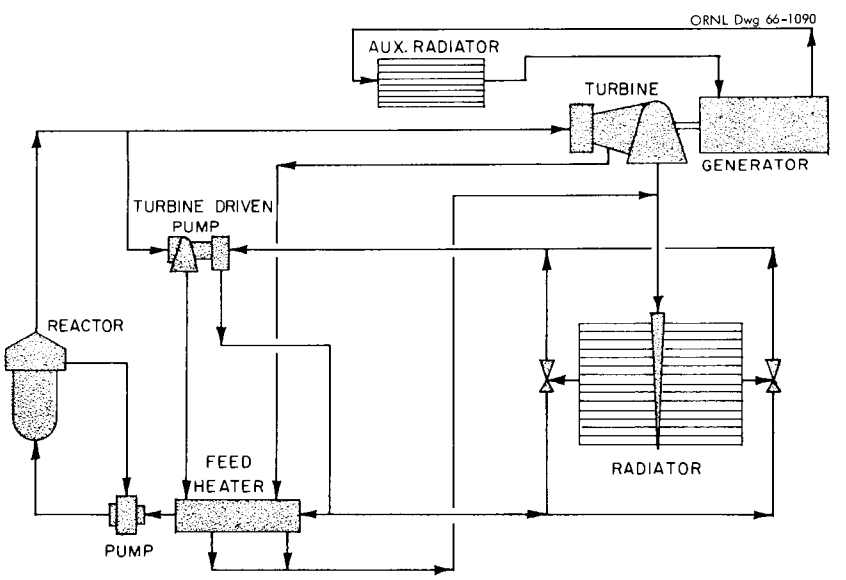


Fig. 9. Simplified Block Diagram of MPRE Boiling-Potassium Circuit.

The vapor separator of the MPRE is designed to yield a vapor quality in excess of 98%. Given this separation, the vapor effluent from the boiler circuit carries with it a negligible fraction of liquid and, as will be argued, negligible solute. The boiler influent (condensate return), on the other hand, is completely liquid and is exposed to stainless steel piping in a temperature range where the acquisition of solute is a certainty. The probability is high, therefore, that more solute will enter the boiler than will leave.

Since the boiler circuit is nearly isothermal, it must quickly become saturated, and conversion of liquid to vapor in the boiler should effect supersaturation, as discussed above. The degree of supersaturation is equivalent to that achieved by evaporating 20% of the liquid less any "dust" suspended in the vapor. Thus although it is a region of maximum temperature, the MPRE boiler is potentially a region of deposition rather than dissolution. The same forces acting to build up solute in the boiler also concentrate impurities in this region. For this reason, oxygen contamination introduced anywhere in the system will eventually migrate to the boiler, and contaminant effects will be felt principally in this region.

As already said, vapor leaving the MPRE boiler carries little or no solute. This follows from the fact that the vapor pressures of known corrosion products are many orders of magnitude less than the equilibrium vapor pressure of potassium at 1540°F. Furthermore, any solute present as "dust" in vapor leaving the boiler would be trapped by the vapor separator. By like token, the potassium vapor should be relatively free of corrosion-inducing impurities. Thus in vapor regions, corrosion either by direct solution or chemical attack should be minimal, and corrosion processes should be principally those associated with sublimation.

Although only a small fraction of liquid escapes the vapor separator, the mass of this liquid integrated over a 10,000-hr period is not inconsequential. If the solute in this liquid were all deposited in the

turbine, operation of this component could suffer. Some dilution of this liquid, however, will inevitably result from heat losses and condensation in the vapor line to the turbine. Also, the MPRE design makes allowance for diverting both sources of liquid into the feed heater through a series of bleeds ahead of and within the turbine. Deposition is therefore not considered a problem in the MPRE turbine.

Because of its low overall solute content, the boiler effluent affords a large driving force for dissolution after condensation. In the MPRE this vapor must first pass through a turbine before reaching the condenser. The work done by the turbine reduces the vapor temperature from 1540 to 1040°F. At the latter temperature, dissolution occurs slowly, as verified in the operation of sodium-cooled reactor plants at 1000°F.

Once condensed, the potassium is sent to a feed heater, where its temperature is increased to approximately 1490°F. The circuit time and relative surface area in this region afford the potassium little opportunity to gain solute, so that the degree of undersaturation of potassium will increase steeply with temperature. Thus the maximum dissolution rate in the MPRE circuit can be expected at the outlet of the feed heater and in the line leading to the boiler jet pump.

At the boiler jet pump, the low-solute condensate return, arriving at a rate of 1 lb/sec, is mixed with saturated boiler liquid, arriving at a rate of 4 lb/sec. Based on the equilibrium solubility curves shown in Fig. 4, the resultant mixture at 1530°F is slightly undersaturated. Assuming perfect mixing, the boiler jet pump would appear free of deposition. In reality, however, the nozzle by which cold potassium enters the jet pump presents a "cold finger" to the saturated boiler liquid. Thus, deposition is possible around the jet pump nozzle. This problem could be further aggravated if deposits carried by the boiler liquid on leaving the boiler find their way through the vapor separator to the jet pump.

In summary, we can regard the MPRE system as subdivided into three basically different corrosion zones: (1) the recirculating boiler, (2) the condenser and condensate return lines, and (3) the vapor lines connecting to and including the turbine. In the first of these zones, the potassium should remain saturated to supersaturated with solute at all points. Hence this first zone should be characterized by deposition rather than corrosion. In contrast, the second corrosion zone, which carries condensate, tends to be highly undersaturated and will be the principal region of dissolutive attack in the system. The third zone, since it is kept virtually free of liquid, will be the least important from a corrosion or deposition standpoint.

## Comparison of Once-Through and Recirculating Boilers

Once-through boilers, in which the liquid is completely dried, differ fundamentally in their corrosion behavior from recirculating-boiler systems. Dissolutive attack in the once-through system occurs not only in the condensate return lines but will continue well up into the boiler. At some point in the boiler, evaporation will cause this liquid to become saturated, and further evaporation to dryness will release all of the contained solute. If the fluid flow conditions are such that the liquid is in the form of a film on the tube walls, deposition will take place near the boiler outlet. On the other hand, if the liquid is in the form of droplets carried with the vapor as a mist, the droplets will evaporate to dryness and the dissolved solids will emerge from the boiler as dust particles. Experience with both water and mercury once-through boilers has shown that either condition may be experienced but the second is more common.[63] Dust will normally collect as hard and adherent deposits in the first stage of the turbine, and in severe cases it may unbalance the turbine rotor as well as restrict vapor flow.

## OPERATING EXPERIENCE WITH CONVENTIONAL ALLOY BOILING SYSTEMS

Among the first development programs conducted in support of the MPRE was an investigation of the corrosion of conventional alloys in boiling potassium. These initial studies used refluxing-potassium capsules, boiling-potassium natural-circulation loops, and boiling-potassium forced-circulation loops incorporating a section containing simulated turbine nozzles and blades. In all cases the primary purpose was to identify potential corrosion problem areas. Differences between each of these tests and the MPRE system were so great as to preclude a direct correlation of corrosion results. Nevertheless, the corrosion trends encountered in these compatibility experiments have proved useful in analyzing the behavior of the MPRE and related systems.

More relevant corrosion data have recently been obtained from a system designed to study fluid flow, boiling flow stability, system control, and corrosion problems of the boiling-potassium reactor system. The basic geometry, surface area ratios, temperature distribution, fluid velocities, and Reynolds numbers were the same as in the MPRE. Examination of the system, however, has been limited to those components that could be removed without undue complication at the end of various stages of the test program.

### Refluxing-Capsule Studies

Table 5 summarizes the results of refluxing-capsule tests operated with conventional alloys and potassium. Figure 10 shows capsule design employed in these studies; one contained tab inserts (Fig. 10a) and the other contained sleeve-type inserts (Fig. 10b). Corrosion of these capsules was encouragingly small (Table 5). Mass transfer profiles for type 316 stainless steel capsules, typified in Fig. 11, revealed slight weight losses in the condensers and slight weight gains in the boilers. Chemical analyses showed these changes to be associated primarily with carbon migration from the condenser to the boiler. The metallographic appearance of a type 316 stainless steel capsule exposed for 1000 hr at 1600°F is illustrated in Fig. 12.

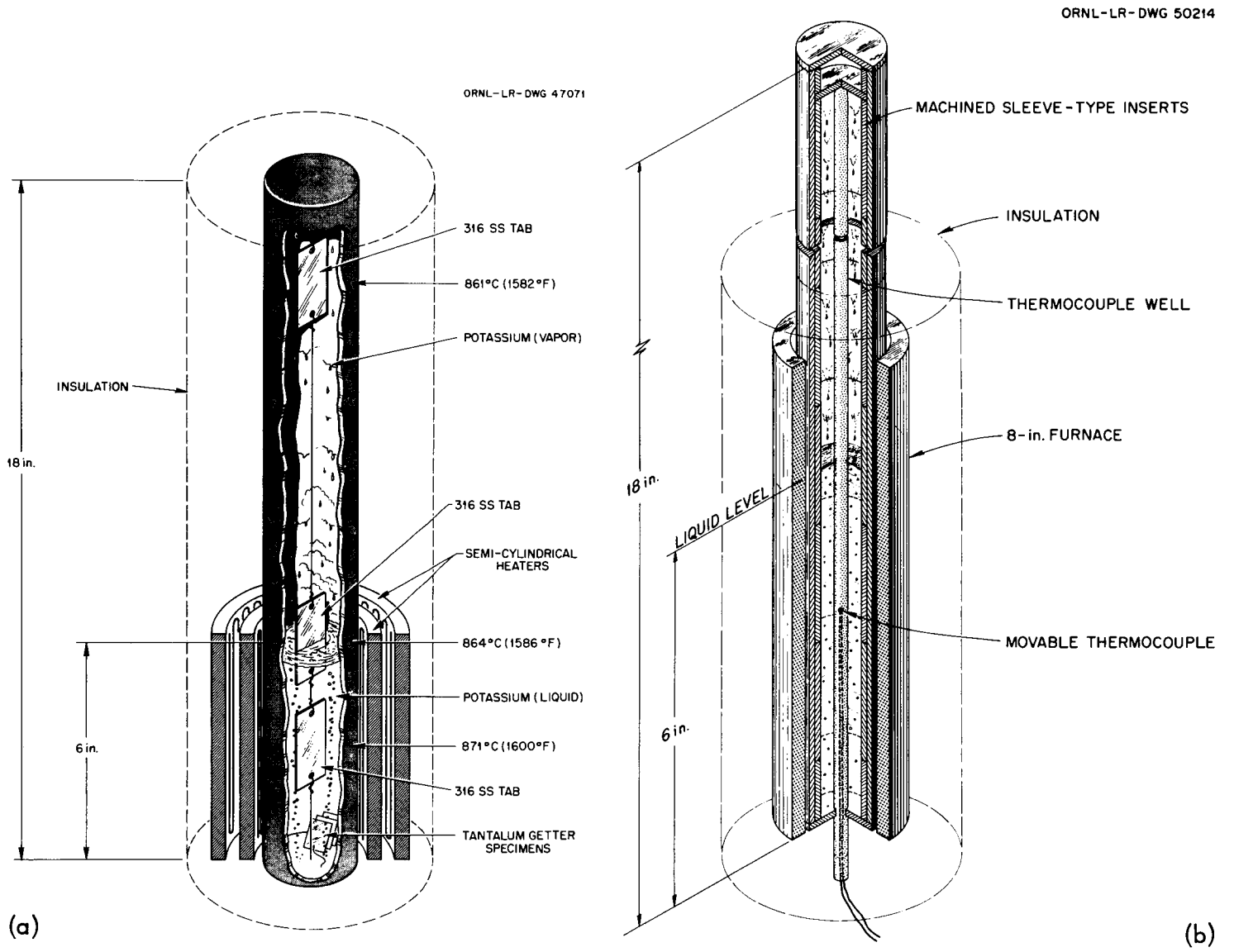


Fig. 10. Configurations of Refluxing Capsules Used to Study Compatibility of Conventional Alloys with Boiling Potassium.

Table 5. Summary of Refluxing Capsule Tests of Boiling Potassium and Conventional Alloys[a]

| Material | | Duration (hr) | Weight Change ($mg/cm^2$) | Metallographic Observations |
|---|---|---|---|---|
| Specimen | Container | | | |
| | Tab Insert Specimens | | | |
| Type 310 stainless steel | Type 310 stainless steel[b] | 500 | +0.31 | No attack |
| Type 316 stainless steel | Type 316 stainless steel[b] | 100 | 0 to +0.6 | No attack |
| Type 316 stainless steel | Type 316 stainless steel[b] | 500 | −0.1 | Surface roughness 1 mil deep |
| Type 316 stainless steel | Type 316 stainless steel | 500 | −0.6 to +0.2 | Surface roughness 1 mil deep |
| Type 316 stainless steel | Type 316 stainless steel[c] | 500 | −0.5 to −0.9 | No attack |
| Inconel | Inconel[b] | 500 | +0.16 to +0.8 | No attack |
| | Sleeve Insert Specimens | | | |
| Type 316 stainless steel | Type 316 stainless steel[c] | 500 | −0.1 to +0.4 | No attack |
| Haynes alloy No. 25 | Haynes alloy No. 25 | 500 | −0.31 to +0.38 | No attack |
| Inconel | Inconel | 1000 | −1.2 to 3.3 | Nonuniform grain boundary attack to 6 mils |
| Type 310 stainless steel | Type 310 stainless steel | 1000 | −1.6 to +6.2 | No attack. Mass transfer deposit in liquid zone |

[a]Capsule temperature: 1600°F boiler, ~1590°F condenser.

[b]With tantalum getter.

[c]Same capsule.

[redacted]



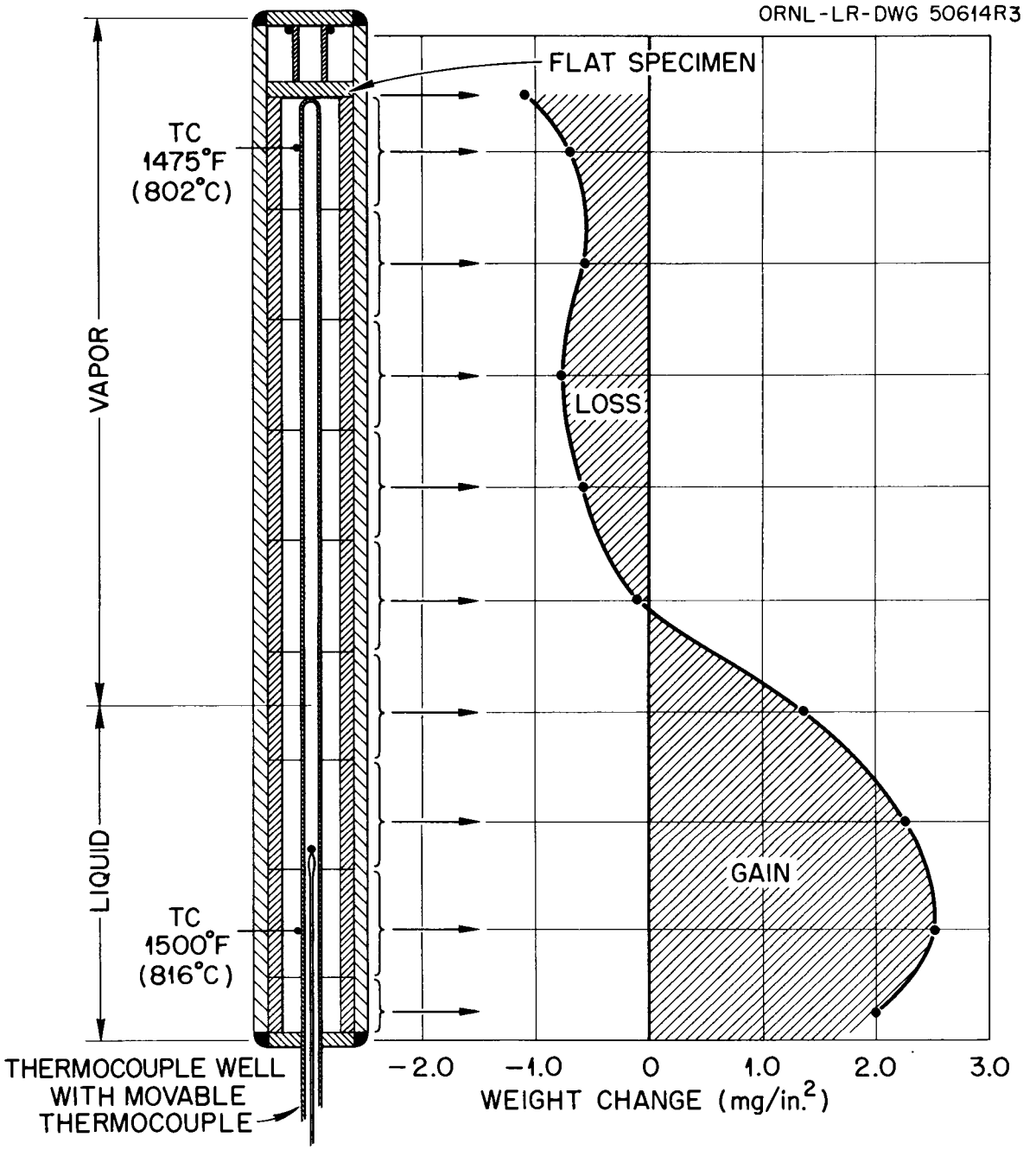


Fig. 11. Weight Losses of Sleeve-Type Inserts in Type 316 Stainless Steel — Refluxing Potassium Capsule Test. Test conditions: 500 hr, boiler temperature: 1600°F.

[redacted]

[redacted]



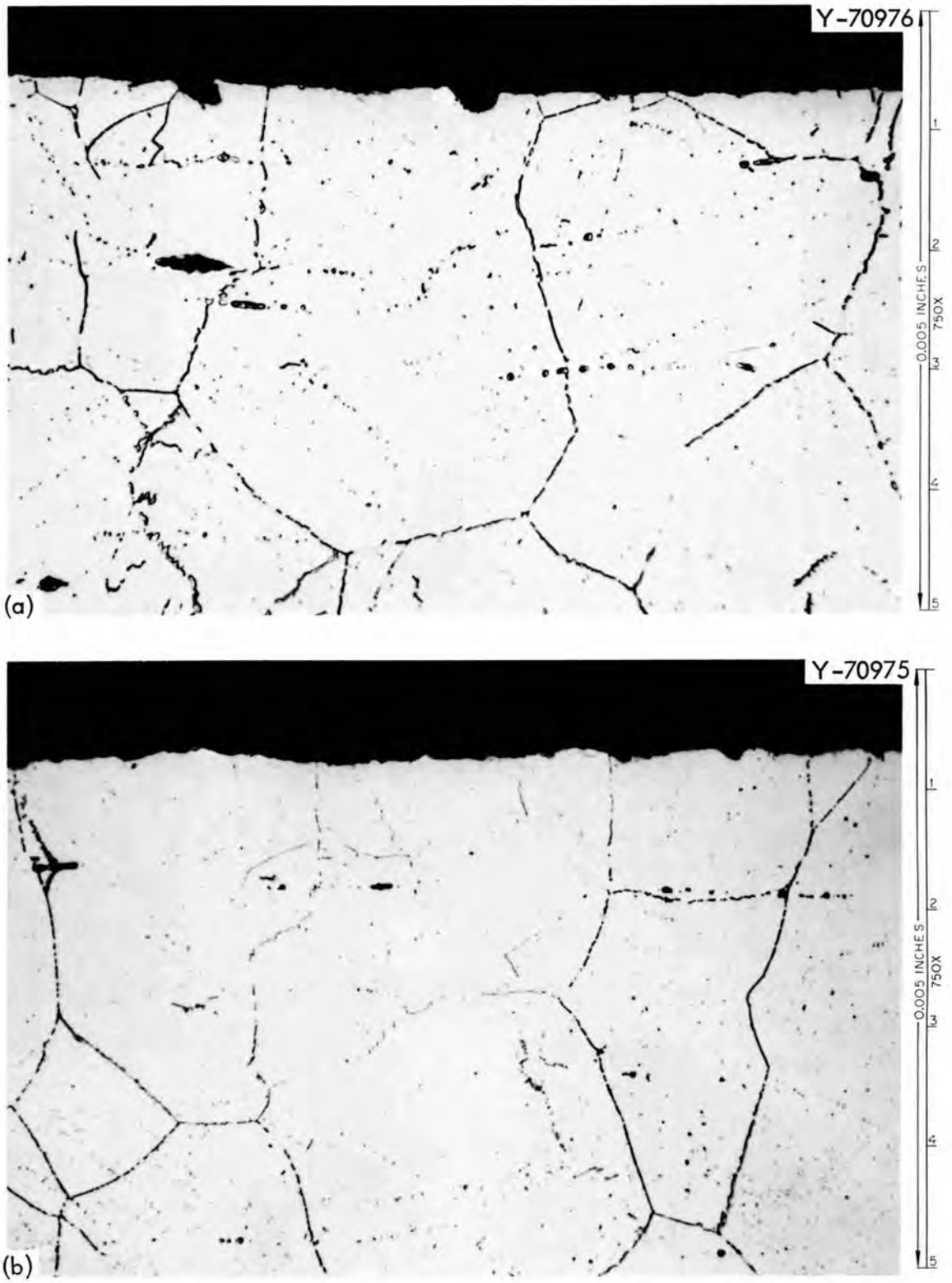


Fig. 12. Metallographic Appearance of Type 316 Stainless Steel Refluxing Capsule Operated for 500 hr at 1600°F. Etchant: lactic acid, $HNO_3$, HCl. 750×. (a) Boiler interface. (b) Condenser interface.

[redacted]

[redacted]



## Natural-Circulation Boiling-Potassium Loops

Following these simple capsule experiments, we operated a series of large natrual-circulation loops of the design shown in Fig. 13.

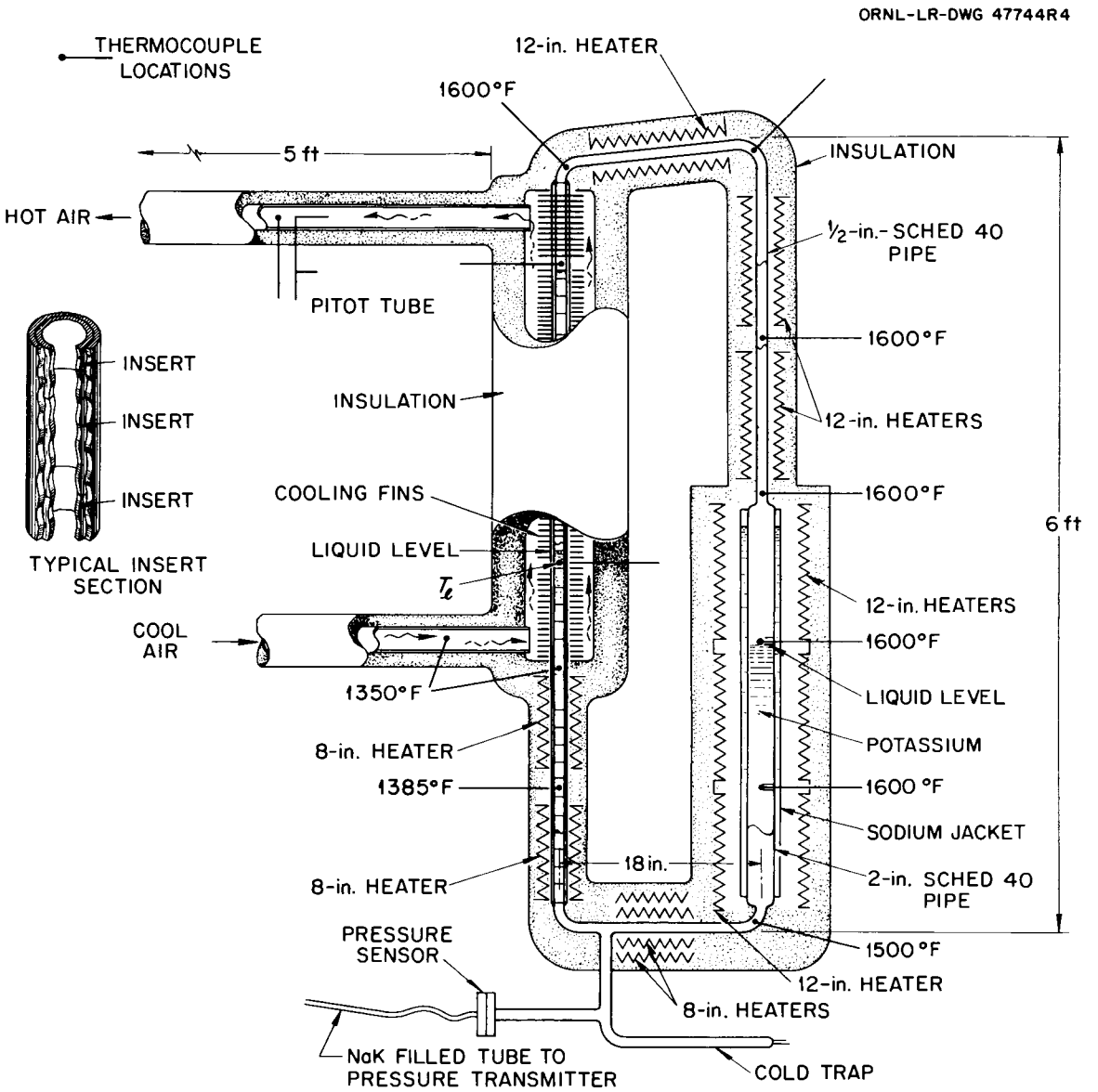


Fig. 13. Natural-Circulation Loop Design Employed to Study Compatibility of Conventional Alloys with Boiling Potassium.

[redacted]

These tests gave the first evidence of liquid superheating and explosive boiling in potassium.[64,65] Although an initial type 316 stainless steel loop operated without difficulty, the next five loops were plagued by severe boiling instabilities, and their analysis was confounded by loop failures caused by thermal fatigue cracking. The operating conditions, corrosion rates, and metallographic results from these tests are summarized in Table 6. The findings, published as a topical report,[27] can be generalized as follows:

1. In tests at 1600°F, type 316 stainless steel and Haynes alloy No. 25 afforded slightly better resistance than Inconel to dissolution by potassium condensate.

2. The condenser inserts of the Haynes alloy No. 25 loop operated at 1800°F lost only slightly more weight than did the ones at 1600°F.

3. Mass transfer deposits were found in the subcooler regions of all loops. In the case of the type 316 stainless steel systems, these deposits were enriched in nickel, chromium, and carbon over the base metal.

4. Carbon migrated in all loops. Surfaces exposed to vapor as well as surfaces in the boiler and condenser lost carbon, while surfaces in the subcooler and preheater regions picked up carbon.

5. Specimens undergoing a loss of carbon showed no difference in short-term mechanical properties from control specimens exposed in argon. However, specimens that gained carbon had somewhat greater strengths and lower ductilities than the control specimens.

Three observations in this series of tests have important ramifications relative to the MPRE. The first concerns the dissolutive attack occurring in condenser sections of the two type 316 stainless steel loops in this series. Both loop condensers operated at a temperature of 1600°F and afforded condensing rates of 0.81 lb $ft^{-2}$ $min^{-1}$. In contrast, the MPRE radiator-condenser operates at only 1040°F and condenses potassium at a rate of 0.44 lb $ft^{-2}$ $min^{-1}$. Though exaggerated compared to the MPRE, condensing conditions in these natural-circulation loops resulted in dissolution rates of type 316 stainless steel inserts below 1 mil/year (Fig. 2).

Table 6. Summary of Conventional Alloy Natural Circulation Loop Test Results

| Loop Material | Test Time (hr) | Temperature, °F | | | Condensing Rate (g/min) | Insert Weight Change | | General Metallographic Results | General Chemical Results |
|---|---|---|---|---|---|---|---|---|---|
| | | Boiler (maximum) | Condenser | Subcooler (minimum) | | Condenser (mg/in.$^2$) | Subcooler (mg/in.$^2$) | | |
| Type 316 stainless steel | 3000 | 1600 | 1600 | 1250 | 180 | | | (a) | (b) |
| Type 316 stainless steel | 3000 | 1670 | 1600 | 1250 | 180 | −8 (uniform) | +90 (maximum) | (c) | (d) |
| Inconel | 1500 | 1600 | 1600 | 1250 | 180 | −8 (uniform) | +50 (maximum) | (e) | (b) |
| Haynes alloy No. 25 | 3000 | 1600 | 1600 | 1250 | 180 | −10 (uniform) | (maximum) | (f) | (d) |
| Haynes alloy No. 25 | 3000 | 1800 | 1740 | 1470 | 300 | −14 (nonuniform) | 70 (maximum) | (g) | (d) |

[a]Subsurface voids at liquid level in boiler 2 mils deep. Surface roughening in condenser approximately 0.5 mil deep.

[b]Transfer of carbon from condenser to subcooler. No preferential removal of Fe, Ni, and Cr from condenser.

[c]Surface roughening to 0.002 in. in boiler. Subsurface voids in condenser 10 to 12 mils deep. Severe cracking in condenser at liquid level. Mass-transfer deposit in subcooler 8 mils deep.

[d]Transfer of carbon from condenser to subcooler.

[e]Intergranular attack to 20 mils in boiler; 5 mils in condenser. Mass-transfer deposit in subcooler 5 mils deep.

[f]Surface roughening in boiler to approximately 0.5 mil. Numerous cracks in boiler at liquid level. Severe cracking in condenser, especially in weld zones. Scattered mass transfer in subcooler 0.5 mil thick.

[g]Surface roughness to <0.5 mil in depth in boiler and condenser. Mass-transfer deposit 7 mils deep in subcooler. Cracks to 28 mils in depth at liquid level in condenser.

A second observation of importance to the MPRE is the presence of metallic deposits in all of the loop systems. The location of these deposits suggests that they were formed by back-diffusion of solute from the pot-type boiler into the subcooler below. Unlike these loops, the boiler region of the MPRE is effectively isothermal; nevertheless, as discussed in the preceding section, deposition may occur in the MPRE boiler. The deposits would be insufficient to threaten plugging except at the jet pump nozzle. However, they could interfere with turbine operation if, under transient flow conditions, they were to surge into strategic locations such as small-clearance bearings.

A final observation of importance to the MPRE concerns the migration of carbon from the condenser and boiler walls to the subcooler. In view of the condensate purity, a similar tendency for decarburization should exist in the MPRE condenser; however, since the latter operates at 1040°F, the rate should be much more sluggish than in these 1600°F loops. Since the MPRE boiler is nearly isothermal, there should be less tendency for temperature gradient mass transfer of carbon than occurred between the boiler and subcooler of these loops.

## Forced-Circulation Boiling-Potassium Loops with Simulated Nozzle-Blade Test Section

The erosion-corrosion resistance of potential turbine blade and nozzle materials for high-temperature potassium is being evaluated in forced-convection loop systems. Two of these facilities have used type 316 stainless steel loops with pot boilers operating at 1600°F.[15,66] The vapor conditions and design of the simulated turbine blade-nozzle test section are shown in Fig. 14. As in the case of the natural-circulation boiling loops described above, initial loops in this series were plagued by boiling instabilities and abnormally high failure rates. Installation of a "hot-finger" boiling nucleation site in later loops eliminated both problems. The test runs completed to date and their operating conditions are summarized in Table 7.

[redacted]



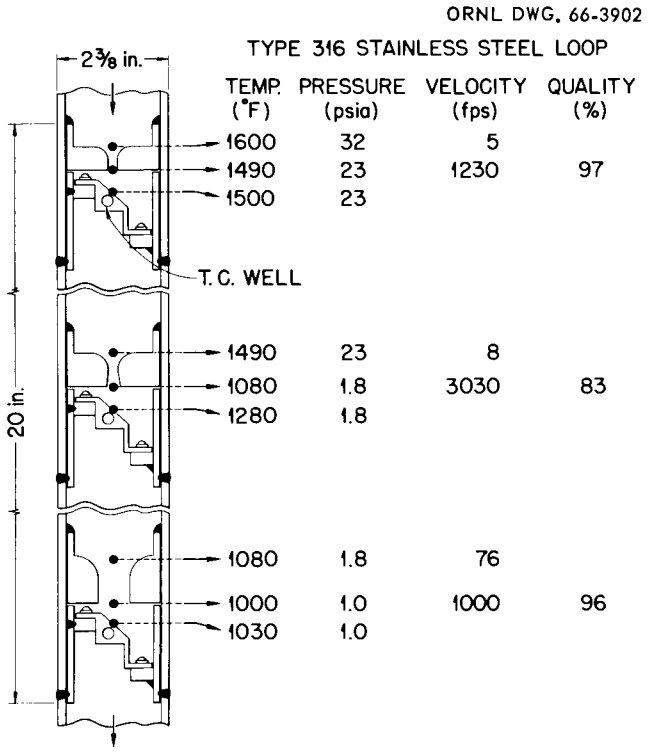


Fig. 14. Nozzle and Turbine Blade Test Section of Boiling-Potassium Corrosion Loop.

Examinations of test sections from these loops revealed the maximum erosion damage in the middle nozzle-blade position with the lowest vapor quality (83%). The first three tests of the TZM alloy resulted in unusually heavy reaction layers and cratering at the impingement areas of the first- and second-stage blades; however, this attack was eliminated in a fourth test by the incorporation of an in-line zirconium hot trap in the boiler preheater. Tests of the other test section alloys revealed little damage beyond formation of a smooth, shallow depression at the second-stage blade impingement area.

Only one complete loop system has been examined to date. Test-section evaluations with this system totaled 3700 hr at a 1600°F boiling temperature. The vapor carry-over line connecting the boiler and test section had been replaced after 500 hr, and the section examined had operated 3200 hr. A schematic drawing of this loop and the metallographic appearance of the various stainless steel sections after test are shown in Fig. 15. Attack was limited to 2.5 mils or less in all regions

[redacted]

Table 7. Summary of Forced-Circulation Loop Tests Conducted in Boiling Potassium-Type 316 Stainless Steel Systems[a]

| Material | | Temperature, °F | | Test Duration (hr) | Examination of Test Section | Reason for Test Termination |
|---|---|---|---|---|---|---|
| Specimen | Container | Maximum | Minimum | | | |
| Type 316 stainless steel | Type 316 stainless steel | 1600 | 1000 | 750 | Second stage turbine blade eroded ~0.001 in. by 3000 ft/sec, 83% quality K vapor | Weld failure at throttling calorimeter line above test section |
| TZM | Type 316 stainless steel | 1570 | | 544 | Severe oxidation of TZM specimens | Failure of Zr hot trap |
| TZM | Type 316 stainless steel | 1500 | | 826 (1st run) | Severe oxidation of TZM specimens | Run 1 shut down for loop modification. Run 2 terminated by thermocouple well failure |
| | | 1600 | 1000 | 1454 (2nd run) | | |
| TZM | Type 316 stainless steel | 1600 | 1250 | 1000 | Severe oxidation of TZM specimens | Scheduled |
| TZM | Type 316 stainless steel[b] | 1600 | 1250 | 1000 | Darkening on blades at impingement area | Scheduled |
| Haynes alloy No. 25 | Type 316 stainless steel | 1550 | | 216 (1st run) | Approximately 20-mil erosion over 1/4-in.-diam region of first stage simulated turbine blade by 1200 ft/sec, 95% quality K vapor | Run 1 shut down for loop modification. Run 2 terminated by heater failure. Run 3 terminated by thermocouple well failure |
| | | 1600 | 1000 | 454 (2nd run) | | |
| | | 1600 | 1000 | 1225 (3rd run) | | |

[a]Condensing rate: 233 g/min; total operating time: 7963 hr.

[b]Contained in-line Zr hot trap.

[redacted]



ORNL-DWG 66-3778

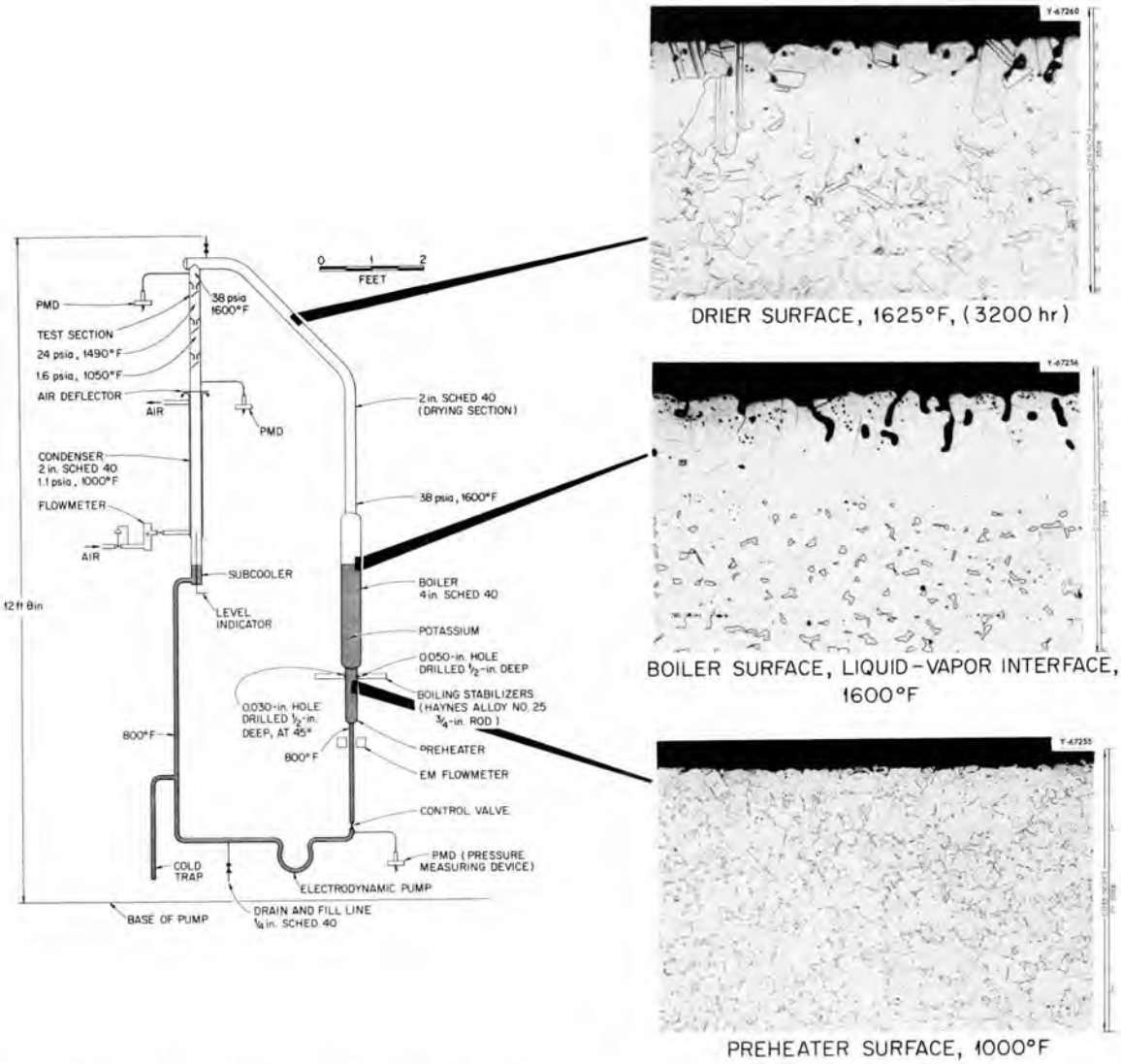


Fig. 15. Surface Condition of Type 316 Stainless Steel from Various Locations of Boiling Potassium Forced Circulation Loop. Etchant: latic acid, HCl, $HNO_3$.

[redacted]

except the liquid-vapor interface in the boiler. The heavier attack in this region was due either to the concentration of impurities occurring from evaporation at the interface or to a hot-spot condition existing near the interface.

## Single-Rod Capsule Tests

Although not designed as corrosion experiments, endurance tests of Firerod electric heaters have provided long-term data on the compatibility of stainless steel with boiling potassium. To evaluate electrical and boiling characteristics, single Firerods clad with either type 304 or 316 stainless steel were tested in boiling potassium in a 2-in.-diam type 316 stainless steel vessel.[67] The Firerods were used as immersion heaters, and vapor generated around the Firerod was condensed at the top of the vessel and refluxed. Each Firerod operated at a nominal power level of 4 kw or 110,000 Btu $hr^{-1}ft^{-2}$. The temperature of the potassium was held in the range 1400 to 1600°F, normally at 1540°F.

These tests have accumulated 86,000 hr of operation and 6 tests have run in excess of 5000 hr each. Figure 16 shows the metallographic appearance of a type 316 stainless steel-clad Firerod that boiled potassium for 8901 hr at 1540°F. All but one of the Firerods examined showed the same limited corrosion effects as this specimen. The one exception was from a test that was found to be highly contaminated with oxygen.

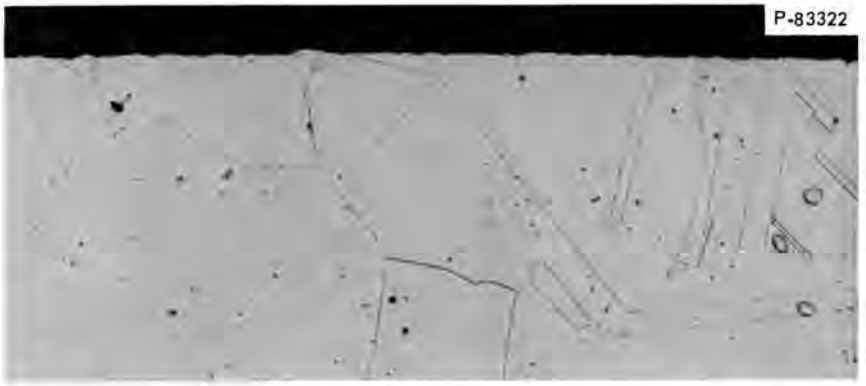


Fig. 16. Appearance of Type 316 Stainless Steel Firerod Cladding After Exposure to Boiling Potassium for 8901 hr at 1540°F.

[redacted]



## Seven-Rod Boiler System (SPS-1)

Figure 17 shows a schematic drawing of the SPS-1 potassium system, which has been used to investigate the operating characteristics of the direct cycle boiling-potassium system.[3] This nonnuclear mockup employs a recirculating boiler heated by a cluster of seven bayonet-type heaters (Firerods). Other major components include a vapor separator, a turbine-driven pump, a condenser-radiator, and boiler and condenser jet pumps.

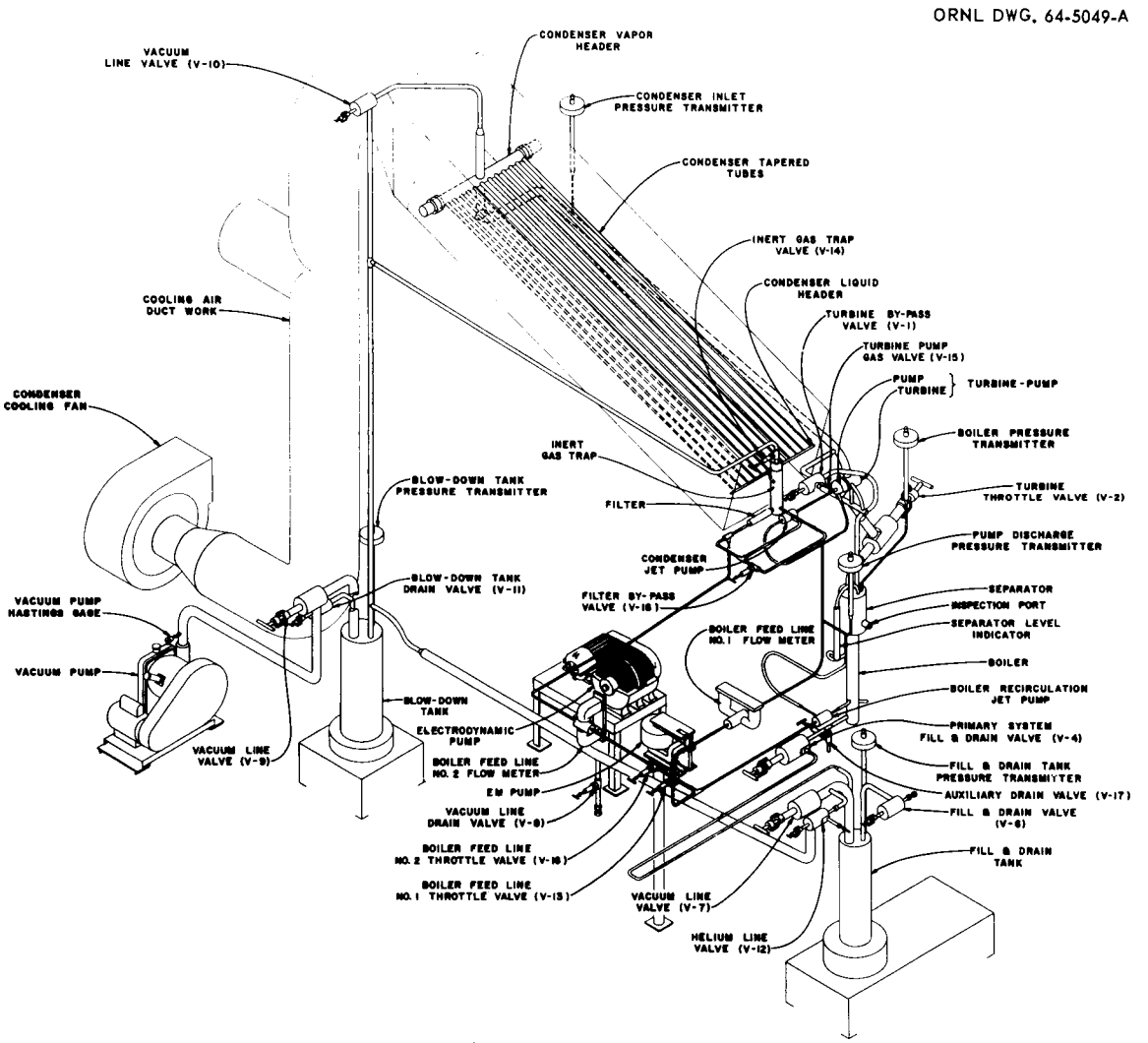


Fig. 17. Schematic Drawing of the Seven-Rod Boiler System (SPS-1).

[redacted]

All components are fabricated of type 316 stainless steel except for the turbine rotor assembly, which is TZM alloy, and the turbine bearings, which are a cobalt-bonded tungsten carbide cermet. Table 8 lists the test runs completed with the SPS-1 system together with the components examined after each run. The results of metallurgical and chemical analyses performed to date are given below.

Table 8. Tests with Seven-Rod Boiler System (SPS-1)

| Test Run | Firerod Bundle | Time at Temperature (hr) | Boiler Temperature (°F) | Power (kw/rod) | Components Examined After Run |
|---|---|---|---|---|---|
| 1 | 1 | 145 | 1300–1500 | ~1.9 | a,b,c,d |
| 2 | 2 | 93 | 1300–1400 | ~1.9 | d |
| 3 | 3 | 30 | 1350–1450 | 2.2 | d |
| 4 | 4 | 10 | 1350–1450 | 1.0–2.0 | d |
| 5 | 4 | 10 | 1350–1450 | 1.0–2.0 | d |
| 6 | 5 | 356 | 1360–1450 | 2.0–3.0 | d |
| 7 | 5 | 690 | 1450–1500 | 2.2–2.5 | a,d |
| 8 | 6 | 433 | 1450–1540 | 2.0–5.0 | a,b,d |
| 9 | 7 | 1521 | 1250–1520 | 1–4.25 | a,b |
| 10 | 8 | 1170 | 1450–1520 | 1–4.25 | a,b,c,e |

[a] Firerods
[b] Boiler jet pump
[c] Condenser jet pump
[d] Pump turbine (housing, blades, bearings, pump impeller)
[e] Condenser tube

Firerod Heaters

Five heater bundles, each consisting of seven Firerods, have been examined following operation in the SPS-1 boiler. Three of the bundles were from tests that operated above 1500°F for times ranging from 1040 to 1520 hr. The other two operated for much shorter times and were exposed to air contamination when the system failed.

The metallographic appearance of the Firerod cladding from the three test runs that exceeded 1000 hr is compared in Fig. 18. Except for carbon migration, none of these Firerods evidenced any measurable corrosive attack. Chemical analyses of the cladding, shown in Table 9, revealed a small carbon increase at the base of the heater and a small carbon loss at the top of the heater. However, these small carbon changes were not manifested by any detectable differences in the distribution of carbide precipitate along the Firerods. This can be seen in Fig. 19, which compares the upper, middle, and lower cross sections of a Firerod from test run 9 (1521 hr).

Table 9. Axial Carbon Profile of Heater Sheaths from SPS-1 Test Runs Exceeding 1000 hr

| Description of Sample | Carbon Content, % | | |
|---|---|---|---|
| | Bundle 5 (Runs 6 and 7) | Bundle 7 (Run 9) | Bundle 8 (Run 10) |
| As-received[a] | 0.065 | 0.030 | 0.030 |
| Top of Heater | 0.040 | 0.018 | |
| Between spacers | | 0.033 | 0.053 |
| Between middle spacer and nucleation rings | | 0.020 | 0.033 |
| Between nucleation rings and taper | 0.034 | 0.035 | 0.042 |
| Bottom of taper | 0.079 | 0.051 | 0.051 |

[a]Vendor's analysis

PHOTO 83059

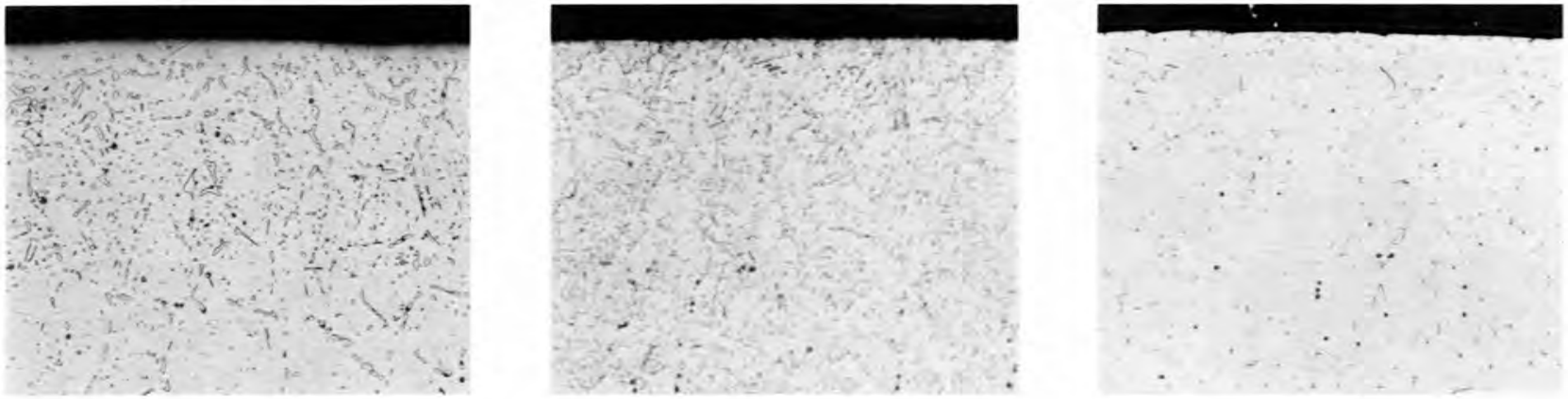


BOILER OUTLET TEMPERATURE: 1450–1540°F

Fig. 18. Photomicrographs of Type 316 Stainless Steel Firerod Cladding After Exposure to Boiling Potassium Seven-Rod Boiler System (SPS-1).

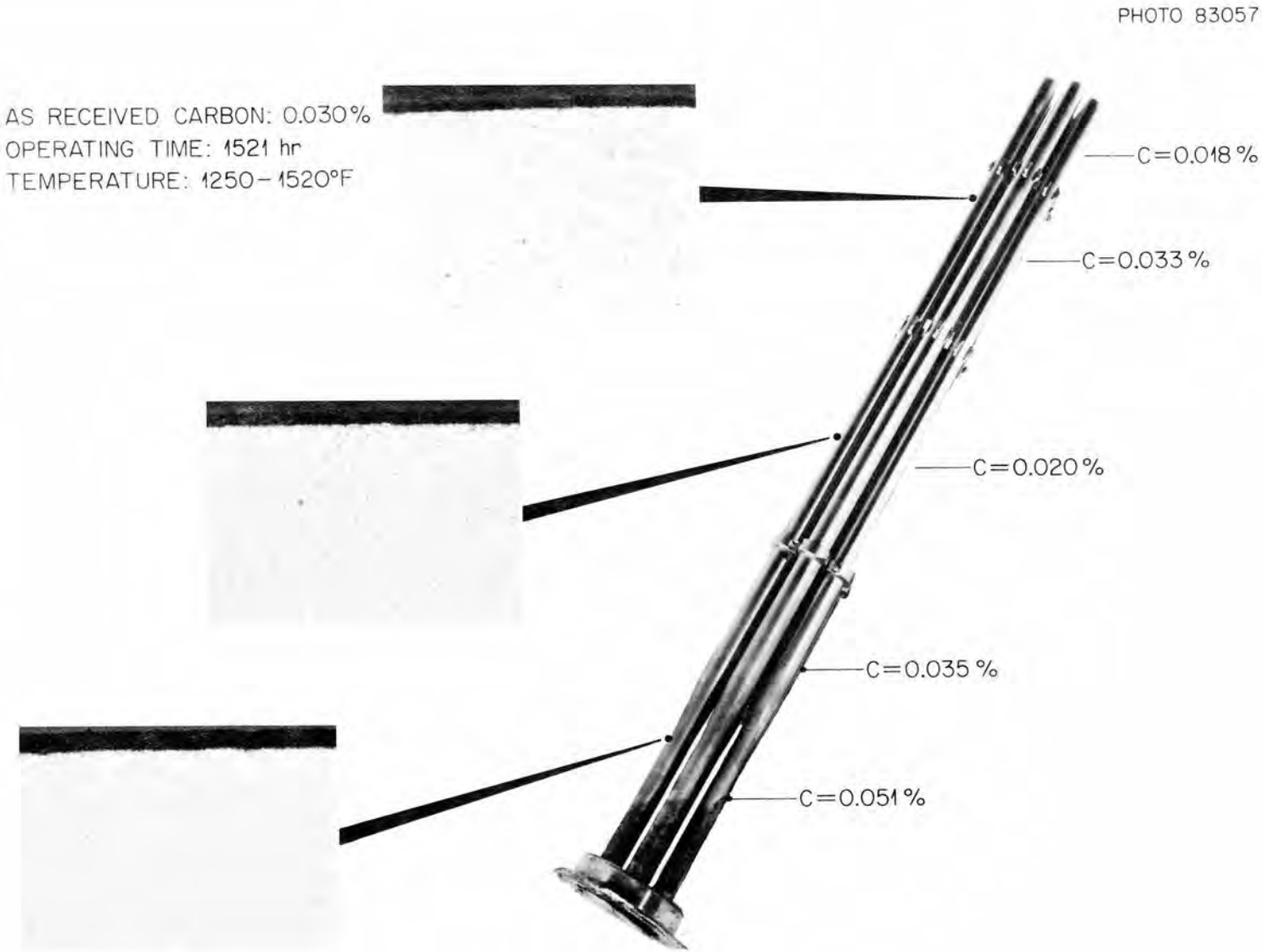


Fig. 19. Appearance of Type 316 Stainless Steel Firerod Cladding from SPS-1 Run 9.

[redacted]



In contrast to these results, the Firerods from test runs 1 and 8 showed 1 to 2 mils of intergranular attack, apparently as a result of exposure to contaminated potassium. Photomicrographs of cladding sections from these two tests are shown in Fig. 20. The first of these test runs was terminated after 145 hr by a "burnout" failure of one of the Firerods[68] and the second was terminated after 433 hr by a heater short in the condensate return line.[69] In view of their relatively short test times and the fact that their operating conditions prior to failure paralleled those of the longer tests, the slight attack suffered by these bundles apparently resulted from the abnormally high oxygen levels that necessarily accompanied each of the containment failures.

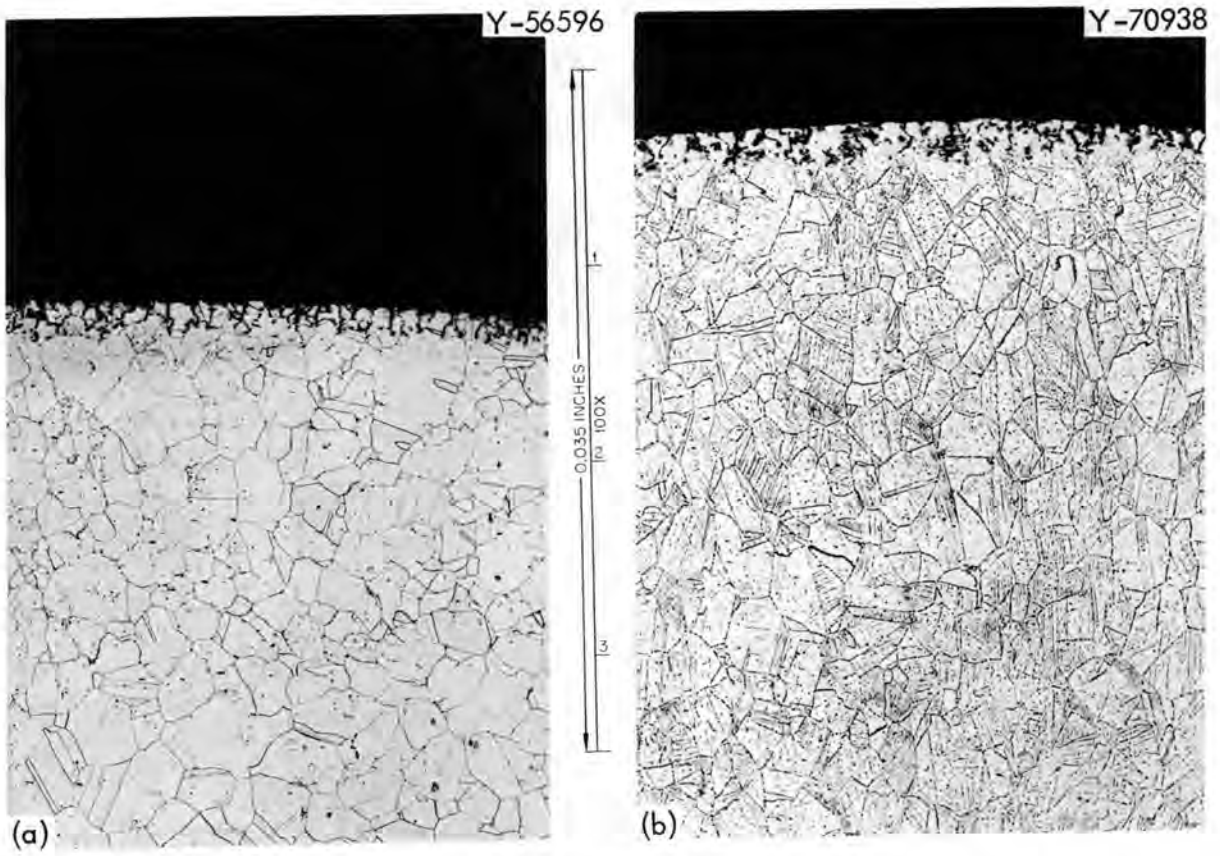


Fig. 20. Photomicrographs of Type 316 Stainless Steel Firerod Cladding, Showing Intergranular Corrosion that Occurred During Test Runs 1 and 8 as a Consequence of Oxide Contamination of the Potassium. (a) Test run 1 operated 146 hr. (b) Test run 8 operated 433 hr.

[redacted]

Boiler Jet Pumps

The SPS-1 boiler feed jet pump was visually inspected following test runs 1, 8, 9, and 10. Runs 1 and 8 had been terminated by containment failures after 145 and 433 hr, respectively. After both runs, mass transfer deposits were found at the top of the nozzle that had injected condensate into the pump and at the pump exit throat leading back to the boiler. The heaviest concentration of deposits occurred during run 8, as shown in Fig. 21. Despite considerably longer operating periods, the boiler jet pumps examined after runs 9 (1521 hr) and 10 (1170 hr) showed no evidence of deposits. The appearance of the pump from run 9 is shown in Fig. 22. Thus, the occurrence of deposits in these pumps, like the intergranular attack of the Firerod cladding, can be traced directly to contamination effects resulting from containment failures.

Fig. 21. Mass Transfer Deposits in Boiler Feed Jet Pump After Oxygen-Contaminated Test Run 8.

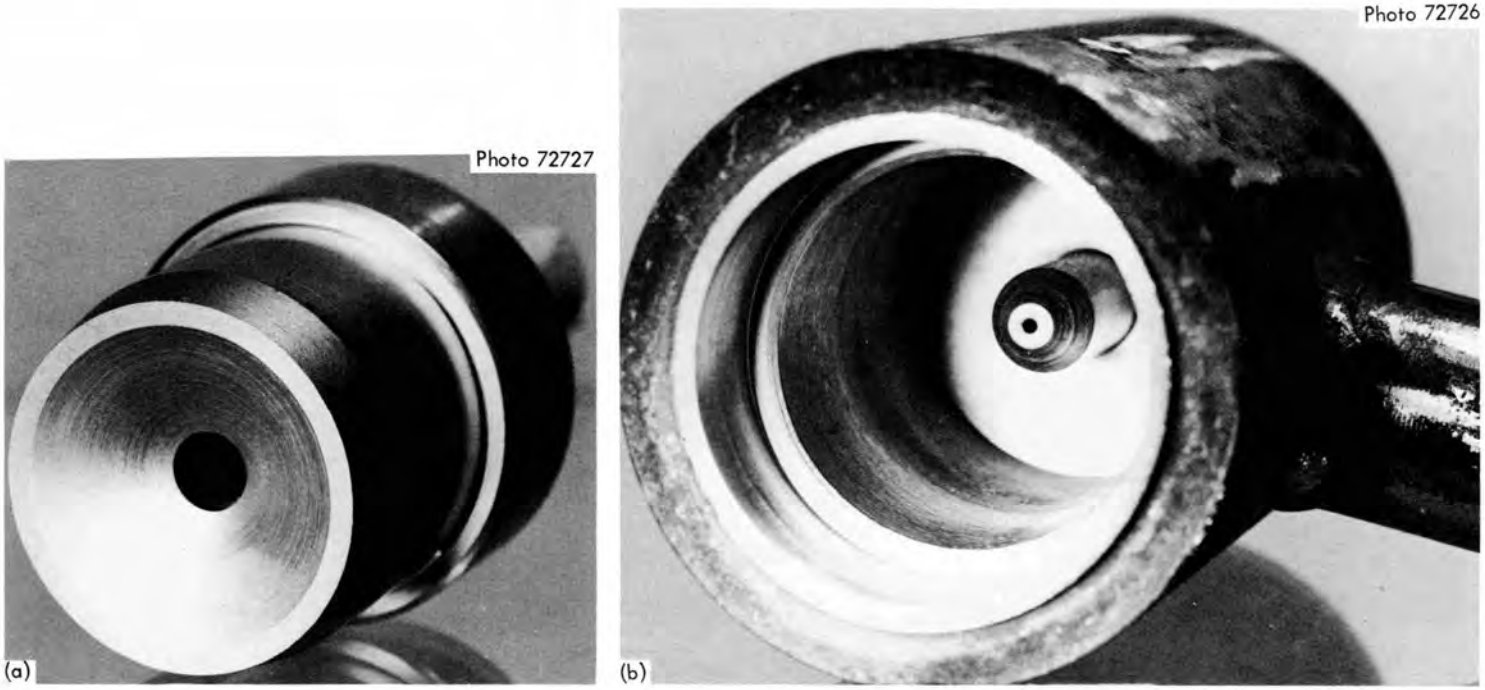


Fig. 22. Boiler Feed Jet Pump Showing Absence of Mass Transfer Products After 1500-hr Exposure in Test Run 9. (a) Jet pump throat. (b) Jet pump nozzle and mixing chamber.

Condenser and Condenser Jet Pumps

The condenser jet pumps were examined only during the initial test runs. No evidence of corrosion was found in this component.

A type 316 stainless steel condenser tube was removed from the SPS-1 system after having completed ten test runs totaling about 4500 hr exposure at 1000 to 1200°F. Cross-section sampling at various points along the tube showed a slight carbon loss at all points:

| Sample Description | Carbon Content (%) |
|---|---|
| As-received | 0.057 |
| Inlet end | 0.046 |
| 10 in. from inlet end | 0.045 |
| 22 in. from inlet end | 0.042 |
| 34 in. from inlet end | 0.042 |
| 46 in. from inlet end | 0.046 |
| 58 in. from inlet end | 0.045 |
| 67 in. from inlet end | 0.047 |

Composite photomicrographs of the condenser tube are shown in Fig. 23. The maximum corrosion, 0.5-mil grain boundary penetration, occurred near the midpoint of the condenser tube. Scattered metallic deposits were also observed in the same region as discontinuous stains which, as shown in Fig. 24, ran along either side of the condenser tube.

The sparse corrosion and deposition in this tube supports the supposition that corrosion rates in the condenser region should be small in view of the relatively low temperature there. The appearance of the deposits suggests that they formed from the evaporation of liquid droplets, which inexplicably did not drain from the fin locations.

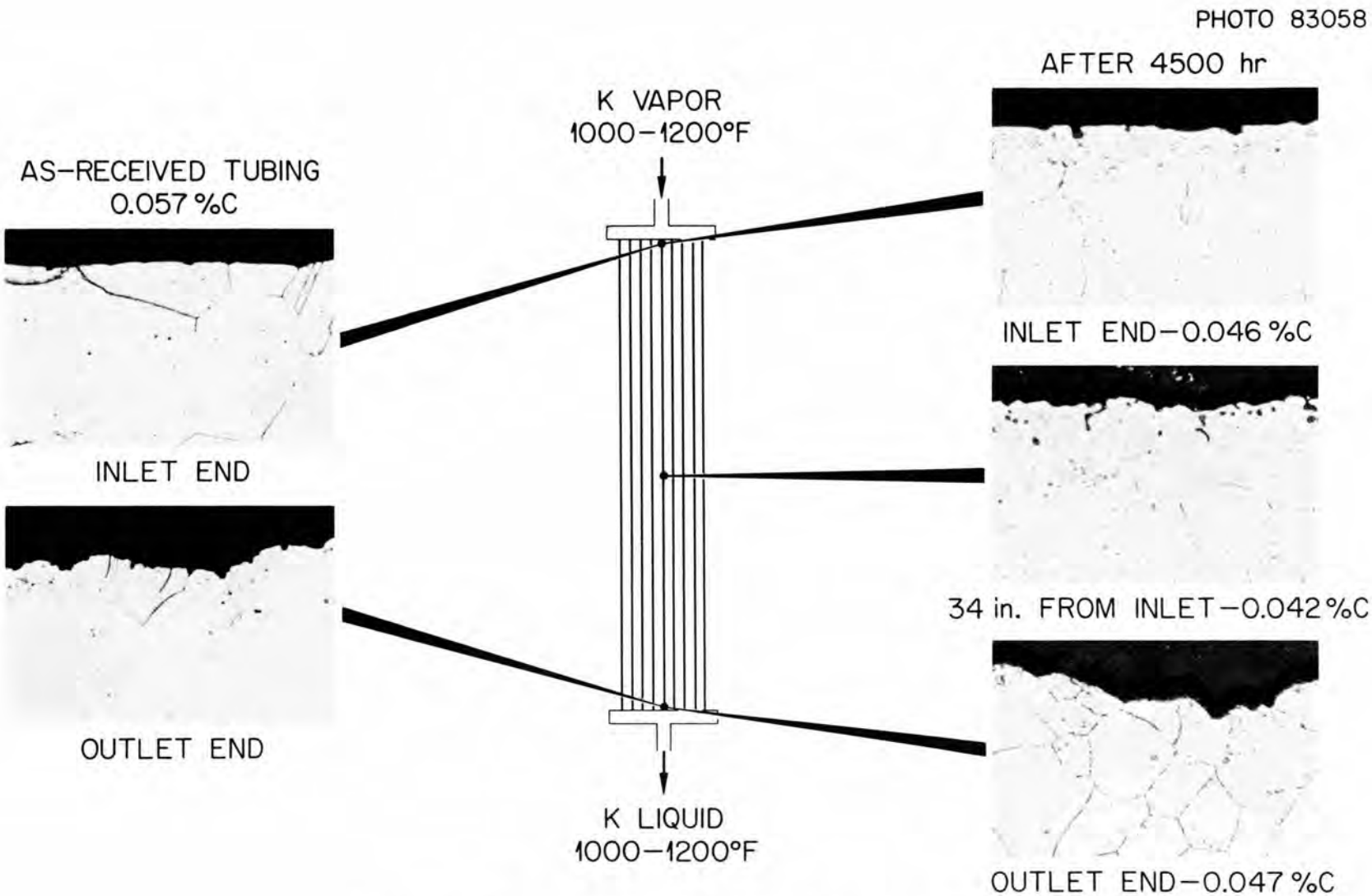


Fig. 23. Appearance of Condenser Tube from SPS-1.

Fig. 24. Longitudinal Section of Condenser Tube Showing Mass Transfer Spotting on Inside Surface.

Turbine-Driven Pump

Turbine-driven pumps were used in the first eight of the ten test runs shown in Table 8. An electromagnetic pump replaced the turbine pump during runs 9 and 10.

The SPS-1 turbine pump is pictured in Fig. 25. The turbines employed a TZM alloy rotary assembly (turbine wheel, shaft, and pump impeller) and cobalt-bonded tungsten carbide bearings. The bearings followed the "hard on hard" principle and were lubricated by potassium. Hydrodynamic lubrication in this relatively small unit required small bearing clearances ranging from 0.0006 to 0.001 in. on the diameter. Visual examinations of these turbines showed the following results.

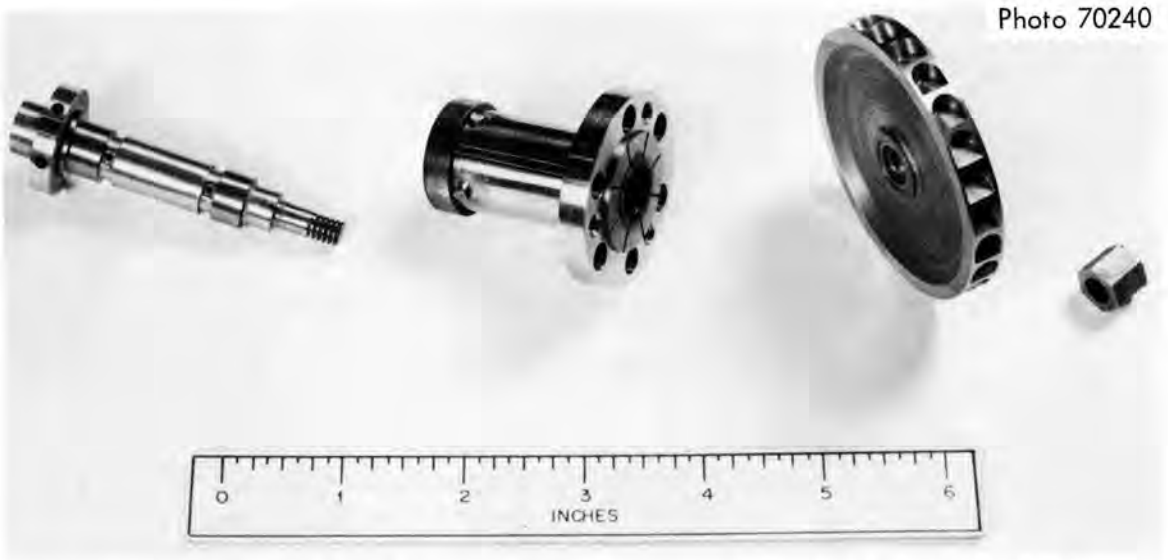


Fig. 25. Turbine-Driven Pump Components Used in Boiler SPS-1.

Turbine Wheel. — No corrosion was observed for any of the turbine blades subjected to potassium vapor at 1540°F, even for operation when significant contamination was present in the boiler (runs 1 and 8). Also, no evidence has been found that mass-transfer deposition had occurred on turbine blade components, although, as mentioned below, some mass-transfer deposits were found on the turbine end of the rotor shaft and radial bearings in one particular test.

Pump Impeller. — No corrosion or erosion damage was evident on any of the pump impellers despite operation in cavitation for greater than 300 hr.

Bearings. — Several test runs of SPS-1 were terminated as a result of turbine bearing seizures resulting from foreign particulates being washed into and ground up by the rotating bearing-shaft assembly.[70,71] Chemical analyses of the foreign debris indicated high concentrations of chromium, manganese, and nickel. One of the chief causes for particulates entering the turbine area was the back-surging of saturated liquid from the boiler, which resulted from transient conditions during system startup or shutdown. However, following test run 6 a mass-transfer deposit was found within recessed grooves on the turbine end of the journal-bearing assembly. Figure 26 shows the location of the deposit on the radial bearing after dissassembly.

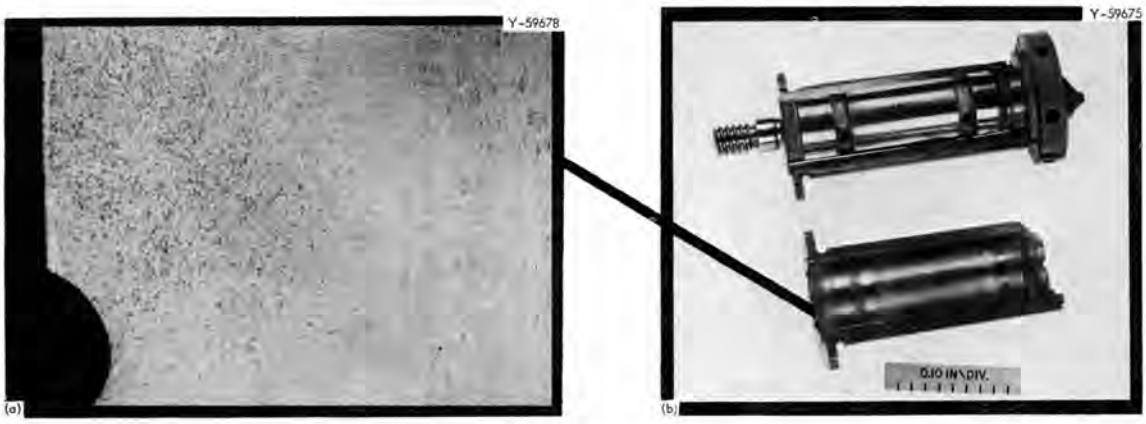


Fig. 26. Mass-Transfer Deposit Within Recess on Turbine-End of Outer Radial Bearing.

Metallurgical examinations of the SPS-1 turbine have confirmed the absence of severe deposition or corrosion problems but have pointed up difficulties associated with the extremely small bearing clearances. The clearance problems of the pump-driven turbine have been eased considerably in the turbine design under test in the Intermediate Potassium System (IPS).[71] Operation of this larger turbine, which employs an 0.003-in. diametral clearance, has now exceeded 2500 hr, and there has been a slight decrease in the starting torque during this period.

## OPERATING EXPERIENCE WITH REFRACTORY-METAL BOILING SYSTEMS

Compatibility studies of refractory metals in boiling potassium have been in progress at ORNL in association with the High-Temperature Materials Development Program.[73] Three types of test facilities have been used for these studies: (1) refluxing-capsule tests, in which dissolution rates are determined at a known condensing rate; (2) natural-circulation loop tests, which provide dissolution and subsequent deposition rates in a condenser and subcooler respectively; and (3) forced-circulation loops designed to investigate mass transfer and corrosion effects in a system with the condenser at a much lower temperature than the boiler, together with the corrosion-erosion resistance of potential nozzle and turbine-blade materials.

Alloys examined to date include Nb–1% Zr, Nb–10% W–1% Zr (D-43), Nb–27% Ta–12% W–1% Zr (FS-85), Ta–8% W–2% Hf (T-111), and Mo–0.5% Ti–0.1% Zr (TZM).

Table 10 summarizes the conditions and results of boiling-potassium capsule and loop tests that have thus far been operated with refractory metals. All tests were conducted under vacuum in the range $10^{-7}$ to $10^{-9}$ torr. The initial oxygen content of the potassium was found to be 70 to 200 ppm by the gettering-vacuum-fusion method[56] and 20 to 50 ppm by the amalgamation method.[74]

Table 10. Summary of Boiling Alkali Metal–Structural Metals Compatibility Tests

| Number of Tests | Material | Fluid | Temperature, °C Maximum | Temperature, °C Minimum | Time per Test (hr) | Condensing Rate (g $min^{-1}$ $cm^{-2}$) | Weight Change ($mg/cm^2$) | Results |
|---|---|---|---|---|---|---|---|---|
| | | | Refluxing Capsules (42,000 hr) | | | | | |
| 5 | Nb–1% Zr | K | 1100–1220 | | 600–5000 | 0.2–0.3 | +0.8 to –0.1 | No evidence of penetration by potassium. Oxygen pickup and migration from top to bottom of capsule |
| 2 | Nb–1% Zr | Na | 1250 | | 5000 | 0.17 | +0.7 to +0.1 | No evidence of penetration |
| 1 | Nb–1% Zr | Rb | 1280 | | 2000 | 0.6 | +0.2 to –0.1 | No evidence of penetration |
| 4 | D-43 | K | 1200–1400 | | 850–5000 | 0.3–0.6 | +1.7 to –0.002 | No evidence of penetration. Oxygen transferred from top to bottom of capsule. Decarburization occurred in areas of high oxygen pickup |
| 1 | TZM | K | 1260 | | 5000 | 0.27 | +7 to –0.4 | Increase in concentration of Ti and Mo in K but no other evidence of attack |
| | | | Natural Circulation Loops (13,000 hr) | | | | | |
| 2 | Nb–1% Zr | K | 1200 | 650 | 1200–2800 | 0.2 | +0.7 to –0.2 | No evidence of penetration. Oxygen pickup in specimens from subcooler region |
| 1 | D-43 | K | 1200 | 835 | 3000 | 0.35 | +0.6 to +0.2 | No evidence of penetration. Oxygen pickup in specimens from subcooler region |
| 1 | T-111 | K | 1250 | 1040 | 3000 | 0.53 | –0.4 to +0.7 | |
| 1 | D-43 Loop/TZM Inserts | K | 1250 | 1040 | 3000 | 0.53 | +0.3 (Av) | No evidence of corrosion. $ZrO_2$ transferred to subcooler. TZM inserts decarburized |
| | | | Forced-Circulation Loops (3000 hr) | | | | | |
| 1 | Nb–1% Zr | K | 1100 | 355 | 3000 | 270 | | 1 mil erosion, second stage blade. Oxygen pickup in boiler and condenser |

Metallographic examination of the boiler and condenser sections from the refluxing-capsule tests disclosed no evidence of dissolutive attack. The expectation of weight losses in the condensing region, reflecting dissolution of the alloy by the condensing vapor, was not realized. Both losses and gains were observed, depending on specimen location in the condenser, but the total gains outweighed the total losses. In those tests with niobium-base alloys, changes in oxygen content were of the same magnitude as the weight changes, so the weight changes appear to be symptomatic of migration of oxygen rather than metal dissolution. Weight changes in a TZM capsule (+7 to −2 $mg/cm^2$) were larger than those found for niobium-base alloys and were more indicative of dissolution, since there was very little evidence of interstitial migration. Both titanium and molybdenum were found in higher than initial concentrations in the potassium after the tests.

The natural-circulation loops revealed corrosion effects that correlated in all respects with the effects observed in corresponding refluxing-capsule tests.[4] That is, weight changes, when corrected for the migration of interstitial elements, showed negligible dissolution of the condenser walls, and there was no evidence of mass transfer of metallic elements to the subcooler.

One Nb–1% Zr forced-circulation loop with Nb–1% Zr nozzle and turbine-blade specimens in the test section has been operated under conditions shown in Table 10. Maximum attack was 1 mil where a 3000-ft/sec stream of 86%-quality vapor impinged on a simulated second-stage turbine blade. No evidence of attack or deposits was found in the boiler, condenser, or subcooler, although chemical analyses of the loop wall showed a slight increase in interstitial oxygen concentration.

## CONCLUSIONS

1. Corrosion rates of stainless steels in liquid sodium and potassium have been determined in forced-circulation loops operated up to 1600°F. Weight losses in these loops indicate less than 1 mil/year uniform wall removal; however, the losses are the result of preferential

leaching of alloying constituents and, in a few cases, intergranular attack. Corrosion rates of stainless steels are quite sensitive to the oxygen level of sodium or potassium.

2. Forced-circulation loop tests of nickel-base alloys in sodium show much higher mass transfer rates above 1300°F than comparable austenitic stainless steel loops. However, corrosion rates of the nickel-base alloys appear less affected by oxygen contamination in the liquid metal.

3. Few data are available on the behavior of cobalt-base alloys in sodium or potassium. The maximum corrosion rate of Haynes alloy No. 25 in a boiling-potassium loop at 1600°F approximated that of a similar type 316 stainless steel loop. The corrosion rate of Haynes alloy No. 25 in a boiling potassium at 1800°F was not substantially higher than at 1600°F.

4. Considerably more data are available on the corrosion resistance of refractory metals in potassium above 2000°F than on cobalt- or nickel-base alloys at 1600 to 1800°F. The refractory metals show very low corrosion rates in boiling sodium and potassium even at 2200°F, provided oxygen levels are in the range established by hot trapping. Mass transfer of interstitial impurities (carbon and nitrogen) occurs at 1300°F and above between niobium or tantalum alloys and conventional alloys in alkali metals.

5. The corrosion mechanisms governing the dissolution of transition metals in sodium and potassium are reasonably well understood. However, solubility and solution-rate data that would permit analysis of mass transfer kinetics are lacking. Furthermore, little attention has been paid to deposition processes, which may be rate limiting in the mass transfer process.

6. Without a basic knowledge of solution and deposition kinetics, simple boiling or nonboiling corrosion experiments cannot be used to gain quantitative data on potassium recirculating boiler systems. Refluxing capsules and natural circulation loops do, however, give insight into the fundamental corrosion processes in boiling-potassium systems. Principal corrosion effects shown by boiling potassium on

stainless steels have been (1) carbon migration, (2) formation of iron-, chromium-, and carbon-rich deposits through supersaturation in the boiler, and (3) modest dissolution rates (< 1 mil/yr) in condenser sections even at 1600°F.

7. The corrosion properties of recirculating boiler systems like the MPRE differ in many respects from those of once-through boilers. The problem of boiler deposits is greater in the once-through system, since all solute picked up by the working fluid between the condenser and boiler is precipitated upon evaporation of the boiler liquid. These deposits are potentially harmful if carried in particulate form by vapor to the turbine. The 20% vapor quality in the MPRE boiler and the use of a vapor separator should minimize the formation and carryover of deposits to the turbine in this system.

8. Consideration of the probable flow rate and concentration profile of solute around the MPRE system indicates that solute should deposit only within the confines of the recirculating boiler and that dissolution should be confined to the condenser and condensate-return lines. The primary problem areas are flow restriction of the boiler jet pump nozzle and dissolution near the feed heater exit. However, operation of subscale engineering mockups of the MPRE has not been affected by either process in the absence of oxygen contamination.

9. Examination of the SPS-1 boiling-potassium system following test runs of 1000 to 1500 hr showed only a slight migration of carbon from the lower sections of the Firerod heater cladding to the top and no evidence of deposits in the boiler jet pump. In shorter test runs that were contaminated by air, Firerod cladding showed 1 to 2 mils of intergranular attack, and the boiler jet pump nozzle was covered by metallic deposits.

10. The turbine-driven pump in the SPS-1 system was affected by the smearing of particulate matter over the bearing surfaces. The particulates apparently entered the pump during back-surges of liquid from the boiler that occurred during shutdowns and startup.

11. A type 316 stainless steel tube removed from the SPS-1 condenser after 4500 hr showed very limited attack (< 0.5 mil). Chemical analyses of the tube indicated a slight loss of carbon near the entrance to the condenser and a slight gain near the bottom.

12. In summary, the corrosion resistance of the 300-series stainless steels appears adequate for service in potassium recirculating-boiling systems to 1550°F, which is the temperature limit set by mechanical property considerations. Nickel- and cobalt-base alloys could, on the basis of high-temperature strength, increase this limiting temperature to 1700°F, but corrosion data are lacking. Refractory metals portend the attainment of service temperatures considerably above 2000°F with less development effort than required for superalloys at more modest temperatures.

[redacted]



REFERENCES

1. A. P. Fraas, The MPRE – A Boiling Potassium Reactor System, AIAA paper No. 64-763 presented at the Third Biennial Aerospace Power Systems Conference, Philadelphia, Pa., September 1–4, 1964.

2. A. M. Perry, Status of MPRE Core Design, paper presented at the AIAA First Rankine Cycle Space Power Systems Specialist Conference, Cleveland, Ohio, October 26–28, 1965 (to be published).

3. R. E. MacPherson and A. P. Fraas, Potassium Rankine Cycle Operating Experience for the Medium Power Reactor Experiment, paper presented at the AIAA First Rankine Cycle Space Power Systems Specialist Conference, Cleveland, Ohio, October 26–28, 1965 (to be published).

4. J. W. Michel and A. M. Perry, Design Study of Boiling Potassium Reactors for Thermal Outputs of 1 Mw to 30 Mw, USAEC Report ORNL-TM-1365, Oak Ridge National Laboratory (to be published).

5. A. P. Fraas and J. W. Michel, Comparison of 1-, 2-, and 3-Loop Systems for Nuclear Turbine-Generator Space Power Plants of 300 Kw to 5 Mw of Electrical Output, USAEC Report ORNL-TM-1366, Oak Ridge National Laboratory, February 1966.

6. G. Samuels, Fuel Element Design for Boiling Potassium Reactors, USAEC Report ORNL-TM-1344, Oak Ridge National Laboratory, January 1966.

7. R. W. Swindeman, Fatigue of Austenitic Stainless Steels in the Low and Intermediate Cycle Range, USAEC Report ORNL-TM-1363, Oak Ridge National Laboratory, January 1966.

8. W. R. Martin, Factors Affecting the Mechanical Properties of Stainless Steels at MPRE Operating Temperatures, USAEC Report ORNL-TM-1362, Oak Ridge National Laboratory, February 1966.

9. K. Goldmann and B. Minushkin, Sodium Technology, Reactor Technology, Selected Reviews – 1965, USAEC Report TID-8541, pp. 321–425.

10. R. W. Harrison, Alkali-Metal Corrosion Studies on Materials for Advanced Space Power Systems, Trans. Am. Nucl. Soc. 8(2): 393 (November 1965).

11. K. Goldmann, N. Hyman, S. Kostman, and J. McKee, Carbon and Nitrogen Transfer in a Type 316 Stainless Steel, Cb–1% Zr Liquid Potassium System, paper presented at the American Nuclear Society Annual Meeting, Washington, D. C., November 15–18, 1965.

12. R. Fox and N. Tumey, MCR Liquid Metal Technology Summary Report, USAEC Report GMAD 3078-32, Vol. I., pp. 4-43, General Motors Allison Division, May 3, 1965.

13. K. Goldmann and B. Minushkin, op. cit., p. 325.

[redacted]

14. L. R. Kelman and R. J. Dunworth, Selection of the Structural Material for the FARET Liquid-Metal Systems, USAEC Report ANL-6939, pp. 10–18, Argonne National Laboratory, December 1964.

15. A. J. Miller, Space Power Progress Reports, USAEC Reports ORNL-3270, pp. 91–104; ORNL-3337, pp. 113–125; ORNL-3420, pp. 221–224 and 235–236; ORNL-3489, pp. 205–206; ORNL-3571, pp. 69–71 and 173–174; and ORNL-3683, pp. 111–112 and 226–230, Oak Ridge National Laboratory.

16. W. H. Jordan et al., Aircraft Nuclear Propulsion Project Progress Reports, USAEC Reports ORNL-1896, pp. 86–87; ORNL-1947, pp. 97–100; ORNL-2012, Part I, II, III, pp. 106–107; ORNL-2061, Part I, II, III, pp. 117–118; ORNL-2106, Part 1–5, p. 135; ORNL-2221, Part 1–5, pp. 175–178; ORNL-2274, Part 1–5, pp. 150–156; ORNL-2340, Part 1–5, pp. 188–189, 214, and 221–222; ORNL-2387, Part 1–5, pp. 222–224; and A. J. Miller, ORNL-2440, Part 1–5, pp. 147, 149, and 176, Oak Ridge National Laboratory.

17. D. M. Donaldson, Compatibility Problems in Fast Reactors, Progr. Nucl. Energy, Ser. IV(5): 102–104 (1963).

18. B. A. Nevsorov et al., Corrosion Resistance of Constructional Materials in Alkali Metals, A/CONF.28/P/343, USSR, paper presented at the Third United Nations International Conference on the Peaceful Uses of Atomic Energy, Geneva, Switzerland, August 31–September 9, 1964.

19. N. Hyman, S. Kostman, and J. McKee, MCR Liquid Metal Technology Summary Report, USAEC Report GMAD 3078-32, Vol. II, pp. 4-69–4-73, General Motors Allison Division, May 3, 1965.

20. R. W. Lockhart and R. S. Young, G.E.-APED Mass Transfer Program, Proceedings of Sodium Components Development Program Information Meeting, Chicago, Illinois, June 16–17, 1965, USAEC Report CONF-650620, p. 23, Division of Technical Information Extension.

21. H. W. Savage et al., SNAP-8 Corrosion Program Summary Report, USAEC Report ORNL-3898, Oak Ridge National Laboratory, December 1965.

22. H. W. Savage, private communications to J. H. DeVan, May 1962.

23. L. Champeix et al., Compatibility of Various Austenitic Steels with Molten Sodium, AEC-tr-6328, paper presented at the Colloquium on the European Society of Atomic Energy on Liquid Metals, Aix-en-Provence, Cadarache, France, September 30–October 2, 1963.

24. D. Gurinsky and C. Klamut, Brookhaven National Laboratory, private communications to J. H. DeVan, October 1964.

[redacted]



25. G. Ilincev, Corrosion Resistance of Stainless Chrome-Nickel Steels in Sodium as a Function of its Oxygen Content, At. Energ. (USSR), 14(4): 375–382 (April 1963).

26. Proceedings of NASA-AEC Liquid-Metals Corrosion Meeting, Lewis Research Center, October 2–3, 1963, USAEC Report NASA SP-41, Vol. I, pp. 213–215, Lewis Research Center, (1964).

27. D. H. Jansen and E. E. Hoffman, Type 316 Stainless Steel, Inconel, and Haynes Alloy No. 25 Natural-Circulation Boiling-Potassium Corrosion Test Loop, USAEC Report ORNL-3790, Oak Ridge National Laboratory, June 1965.

28. J. R. DiStefano and E. E. Hoffman, Corrosion Mechanisms in Refractory Metal-Alkali Metal Systems, USAEC Report ORNL-3424, pp. 26–39, Oak Ridge National Laboratory, August 1963.

29. A. P. Litman, The Effect of Oxygen on the Corrosion of Niobium by Liquid Potassium (Thesis), USAEC Report ORNL-3751, Oak Ridge National Laboratory, July 1965.

30. J. R. DiStefano and A. P. Litman, Effects of Impurities on Some Refractory Metal–Alkali Metal Systems, Corrosion, 20(12): 392–399 (1964).

31. A. J. Romano, R. H. Fleitman, and C. J. Klamut, Summary of the High-Temperature Alkali Metal Corrosion Program at Brookhaven National Laboratory, AEC-NASA Liquid Metals Information Meeting, Gatlinburg, Tennessee, April 21–22, 1965, USAEC Report CONF-650411, Division of Technical Information Extension (in press).

32. J. H. DeVan, J. R. DiStefano, and D. H. Jansen, Compatibility of Refractory Metals with Boiling Alkali Metals, Trans. Am. Nuc. Soc. 8(2): 390–391 (1965).

33. J. R. DiStefano and E. E. Hoffman, A Survey of the Compatibility of Some Potential Refractory-Metal Fuel Cladding Materials with Potassium, USAEC Report ORNL-TM-708, pp. 7–18, December 1963.

34. R. L. Ammon, R. W. Buckman, Jr., and T. Begley, Tantalum Base Alloys for Alkali Metal Containment, Trans. Am. Nucl. Soc. 8(2): 401–402 (1965).

35. W. D. Manly, Fundamentals of Liquid-Metal Corrosion, Corrosion, 12(7): 336–342 (1956).

36. E. A. Moelwyn-Hyghes, The Kinetics of Reactions in Solution, p. 374, Oxford Univ. Press, London, 1947.

[redacted]

37. A. G. Ward and J. W. Taylor, Solution Rate Studies with Liquid Metals, British Atomic Energy Report AERE M/R 1866, 1956.

38. W. R. Holman, Mass Transfer in High Temperature Sodium Loops, Nucl. Sci. Eng. Suppl. 2(1): 27–28 (1959).

39. S. W. Strauss, J. L. White, and B. F. Brown, The Atomic Size Effect and Alloying Behavior in Liquid Metals, Acta Met., 6(9): 604–606 (1958).

40. H. W. Leavenworth and R. E. Cleary, The Solubility of Ni, Cr, Fe, Ti, and Mo in Lithium, Acta Met., 9(5): 519–520 (1961).

41. J. H. Hildebrand and R. L. Scott, The Solubility of Non-electrolytes, pp. 27, 270, Reinhold Publishing Corp., New York, 1955.

42. J. H. Swisher, The Solubility of Iron, Nickel, and Cobalt in Liquid Potassium and the Effect of Oxygen Gettering Agents on Iron Solubility, NASA Report NASA-TN-2734, Lewis Research Center, March 1965.

43. C. B. Jackson, Liquid Metals Handbook, Sodium (NaK) Supplement, p. 15, U.S. Government Printing Office, Washington, D. C., 1955.

44. S. J. Rodgers, L. W. Mausteller and E. F. Batutis, Iron and Nickel Concentrations in Sodium, NAS Tech. Rep. 27, Mine Safety Appliances Company, Callery, Pa., June 30, 1954.

45. R. L. McKisson and R. L. Eichelberger, Solubility Studies of Ultra Pure Transition Elements in Ultra Pure Alkali Metals, Seventh Quarterly Report, NASA Report NASA-CR-54097, AI-65-93, Atomics International, June 1965.

46. W. S. Ginell and R. J. Teitel, Solubility of Transition Metals in Molten Potassium, AEC-NASA Liquid Metals Information Meeting, Gatlinburg, Tennessee, April 21–22, 1965, USAEC Report CONF-650411, Division of Technical Information Extension (in press).

47. R. E. Cleary, S. S. Blecherman, and J. E. Corliss, Solubility of Refractory Metals in Lithium and Potassium, USAEC Report TIM 850, Pratt and Whitney, CANEL, October 27, 1965.

48. A. P. Litman, op. cit., p. 82.

49. C. Tyzack, The Behavior of Meterials in Liquid Sodium, Advances in Materials (Inter-Disciplinary Symposium), The Institution of Chemical Engineers, London, 1964.

50. G. W. Horsley, The Corrosion of Iron by Oxygen-Contaminated Sodium, British Atomic Energy Report AERE M/R 1441, April 1964.

51. G. W. Horsley, Corrosion of Iron by Oxygen-Contaminated Sodium, J. Iron Steel Inst. (London), 182: 43 (1956).

52. L. F. Epstein, Chem. Eng. Progr. Symp. Ser., 53: 67 (1957).

53. M. Davis and A. Draycott, Compatibility of Reactor Materials in Flowing Sodium, Proc. U. N. Intern. Conf. Peaceful Uses At. Energy, 2nd, Geneva, 1958, 7: 97–98 (1958, 1959).

54. B. R. T. Frost, Advances in Liquid Metal Technology, J. Nucl. Mater., 7(2): 116 and 121 (1962).

55. E. M. Simons and J. F. Tagedrost, Mass Transfer of TZM Alloy by Potassium in Boiling-Refluxing Capsules, AEC-NASA Liquid Metals Information Meeting, Gatlinburg, Tennessee, April 21–22, 1965, USAEC Report CONF-650411, Division of Technical Information Extension (in press).

56. A. P. Litman and J. W. Prados, The Partitioning of Oxygen Between Zirconium and Liquid Potassium, Electrochem. Technol., 3(9-10): 228–233 (1965).

57. V. S. Lyashenko and B. A. Nevzorov, Corrosion Reactor Mater., Proc. Conf., Salzburg, Austria, 1962, 2: 365 (1962).

58. W. J. Anderson and G. V. Sneesby, Carburization of Austenitic Stainless Steels in Liquid Sodium, USAEC Report NAA-SR-5282, Atomics International, September 1960.

59. D. D. Williams, Solubility of Oxygen in Potassium Metal and Sodium-Potassium Alloys, USAEC Report NRL-3894, Naval Research Laboratory, December 1951.

60. D. D. Williams, J. A. Grand, and R. R. Miller, Determination of the Solubility of Oxygen-Bearing Impurities in Sodium, Potassium and their Alloys, J. Phys. Chem., 63(1): 68 (1959).

61. C. Tyzack, The Corrosion of Iron and Steel in Liquid Sodium, Steels for Reactor Pressure Circuits, Iron Steel Inst. (London) Spec. Rep., 69: 179–195 (1961).

62. D. Kirkbride, Los Alamos Scientific Laboratory, private communications to J. H. DeVan, March 1966.

63. J. F. Nejedlik, Mecury Materials Evaluation and Selection, SNAP-2 Power Conversion System Topical Report No. 24, NASA Report TRW ER-5643, NAA-SR-6316, p. 85, Thompson Ramo Wooldridge, March 1964.

64. H. W. Hoffman and A. I. Krakoviak, Convective Boiling with Liquid Potassium, pp. 19–37 in Proceedings of 1964 Heat Transfer and Fluid Mechanics Institute, ed. by W. H. Guiet and S. Levy, Stanford University Press, Stanford, Calif., 1964.

65. J. A. Edwards and H. W. Hoffman, Superheat with Boiling Alkali Metals, Proceedings of Conference on Application of High Temperature Instrumentation to Liquid Metal Experiments, USAEC Report ANL-7100, Argonne National Laboratory (in press).

66. A. P. Fraas, Medium-Power Reactor Experiment Quarterly Progress Reports, USAEC Reports ORNL-3818, pp. 125–129; ORNL-3860, pp. 78–82; and ORNL-3897, pp. 96–98, Oak Ridge National Laboratory.

67. A. P. Fraas, Medium-Power Reactor Experiment Quarterly Progress Reports, USAEC Reports ORNL-3818, pp. 35–40 and ORNL-3860, pp. 21–25, Oak Ridge National Laboratory.

68. N. C. Cole and C. E. Sessions, pp. 93–96, Space-Power Program Semiann. Progr. Rept. June 30, 1964, USAEC Report ORNL-3683, Oak Ridge National Laboratory.

69. A. P. Fraas, Medium-Power Reactor Experiment Quarterly Progress Reports, USAEC Reports ORNL-3860, pp. 26–34, and ORNL-3897, pp. 100–105, Oak Ridge National Laboratory.

70. A. J. Miller, pp. 65–80, 93–102, Space-Power Program Semiann. Progr. Rept. June 30, 1964, USAEC Report ORNL-3683, Oak Ridge National Laboratory.

71. A. P. Fraas, Medium-Power Reactor Experiment Quarterly Progress Reports, USAEC Reports ORNL-3774, pp. 41–46, 102–107, and ORNL-3818, pp. 41–51, 134–139, Oak Ridge National Laboratory.

72. J. Zasler et. al., Medium-Power Reactor Experiment Quarterly Progress Reports, USAEC Reports ORNL-3897, pp. 70–77, and ORNL-3937 (in press), Oak Ridge National Laboratory.

73. W. C. Thurber, High-Temperature Materials Program Quarterly Progress Reports, USAEC ORNL-TM-980, pp. 56–65, 67–71; ORNL-TM-1050, pp. 41–50; W. C. Thurber and W. O. Harms, ORNL-TM-1140, pp. 29–40; W. O. Harms, ORNL-TM-1300, pp. 25–34; and ORNL-TM-1350, pp. 27–49, Oak Ridge National Laboratory.

74. L. P. Pepkowitz and W. C. Judd, Anal. Chem. 22(10): 1283–1286 (1950).

## INTERNAL DISTRIBUTION

1–2. Central Research Library
3. Reactor Division Library
4. ORNL Y-12 Technical Library
Document Reference Section
5–24. Laboratory Records Department
25. Laboratory Records, ORNL R.C.
26. ORNL Patent Office
27. G. M. Adamson
28. S. E. Beall
29. M. Bender
30. G. E. Boyd
31. H. C. Claiborne
32. N. C. Cole
33. E. L. Compere
34. W. H. Cook
35. W. B. Cottrell
36. F. L. Culler
37. C. W. Cunningham
38. J. E. Cunningham
39–48. J. H. DeVan
49. J. R. DiStefano
50. D. A. Douglas
51. B. Fleischer
52. J. Foster
53. C. W. Fox
54–73. A. P. Fraas
74. J. H Frye
75. L. C. Fuller
76. W. R. Grimes
77. A. G. Grindell
78. P. N. Haubenreich
79. W. O. Harman
80. M. R. Hill
81. H. W. Hoffman
82. W. R. Huntley
83. D. H. [illegible]sen
84. S. I. [illegible]aplan
85. P. [illegible] Kasten
86. J. [illegible] Keyes
87. R. B. Korsmeyer
88. [illegible] E. Lackey
89. [illegible]. E. LaVerne
90. A. P. Litman
[illegible] D. Lloyd
[illegible]. M. I. Lundin
93. R. N. Lyon
94. H. G. MacPherson
95. R. E. MacPherson
96. W. R. Martin
97. H. C. McCurdy
98. J. W. Michel
99. A. J. Miller
100. P. Patriarca
101. A. M. Perry
102. G. Samuels
103. A. W. Savolainen
104. J. L. Scott
105. C. E. Sessions
106. G. M. Slaughter
107. O. L. Smith
108. I. Spiewak
109. G. M. Tolson
110. D. B. Trauger
111. A. M. Weinberg
112. J. R. Weir, Jr.
113. G. D. Whitman
114. J. [illegible]. Wilson
115. F. W[illegible]nslow
116. M. M. [illegible]arosh
117. Gale Y[illegible]ng
118. J. Zasle[illegible]

## EXTERNAL DISTRIBUTI[illegible]

119. C. H. Armbruster, Wrig[illegible] Development Center, Dayton, Ohio
120. D. Blancher, Lockheed [illegible]nk, California
121. R. S. Carey, Aeroje[illegible] Gener[illegible] Corp., Azusa
122. G. K. Dicker, AEC Washingto[illegible]
123. Sherman Edwards, Lockheed, Sacra[illegible]to, California

[redacted]

[redacted]



124–133. H. B. Finger, AEC, Washington
134. R. Fox, Allison Division, General Motors, Indianapolis
135. D. H. Grinsky, Brookhaven National Laboratory
136. Graham Hurley, NASA, Houston
137. E. E. Hoffman, Missile and Space Div. General Electric Co., Evendale, Ohio
138. Carl E. Johnson, AEC, Washington
139. J. D. Lafleur, AEC, Washington
140–144. Bernard Lubarsky, NASA, Lewis Research Center
145. James Lynch, NASA, Washington
146. T. A. Moss, NASA, Lewis Research Center
147. M. Parkman, Aerojet-General Corp., Azusa
148. Benjamin Pinkel, Douglas Corp., Santa Monica, California
149. Louis Rosenblum, NASA, Lewis Research Center
150. A. J. Rothman, Lawrence Radiation Laboratory, Livermore
151. Abe Silverstein, NASA, Lewis Research Center
152. J. M. Simmons, AEC, Washington
153–157. R. M. Spencer, AEC, Washington
158. Jack Stearns, JPL, Pasadena, California
159. H. J. Stewart, JPL, Pasadena, California
160. G. C. Szego, IDA, Arlington, Virginia
161. M. J. Whitman, AEC, Washington
162. T. F. Widmer, RCA, Valley Forge, Philadelphia, Pennsylvania
163. Gordon Woodcock, NASA, Huntsville
164. W. Woodward, NASA, Washington
165–179. Division of Technical Information Extension
180. Research and Development Division, AEC, Oak Ridge Operations
181–182. Reactor Division, AEC, Oak Ridge Operations

[redacted]